TRANSFER PATH ANALYSIS ON A HEAVY-DUTY TRUCK AND A NOVEL FORCE IDENTIFICATION APPROACH

by

Andrei-Cristian STAN

A Thesis Submitted to the
Graduate School of Engineering
in Partial Fulfillment of the Requirements for
the Degree of

Master of Science
in
Mechanical Engineering

April 2015
Koc University
Graduate School of Sciences and Engineering

This is to certify that I have examined this copy of a master's thesis by

Andrei-Cristian STAN

and have found that it is complete and satisfactory in all respects,
and that any and all revisions required by the final
examining committee have been made.

Committee Members:

____

Ipek Basdogan, Ph. D.

____

Murat Sözer, Ph. D.

____

Kenan Şanlıtürk, Ph. D.

Date: ________________________

ABSTRACT

TRANSFER PATH ANALYSIS ON A HEAVY-DUTY TRUCK AND A NOVEL FORCE IDENTIFICATION APPROACH

Most of the mechanical systems are composed of different subsystems coupled by several links. Any excitation acting on the system is divided into several internal forces which propagate through these links or so called transfer paths. This thesis presents the use of experimental Transfer Path Analysis (TPA) in identifying the transmission paths and their contribution for a heavy duty truck in order to estimate the vibration and noise transmitted from the cabin and engine mounts. TPA uses the operating forces to calculate the response by multiplying them with the corresponding transfer functions. For that reason, predicting the operating forces accurately have become a major research topic and can be done using different methods. One of the methods that is commonly used is called "matrix inversion method" and it is used when the transfer paths include rigid connections or the mounts are very stiff compared to the receiving structure. When matrix inversion methods are used, the errors in the experimental measurements and poor conditioning can often lead to unreliable results.

This thesis focuses on developing new techniques to improve the force identification process in TPA. The required data for TPA is measured on a heavy duty truck. The operating response values at the desired locations (steering wheel accelerations and sound pressure level inside the cabin) are also measured on the truck to verify the validity of the predicted values. First, classical TPA method is employed in order to predict the sound pressure level inside a prototype heavy duty truck cabin and the vibration level on the steering wheel. To validate the predicted results, coherence of the collected data and the condition numbers of FRF matrices are investigated so that the accuracy of the predicted results can be quantified for the frequency band of interest. The predictions of the total response are compared with the experimentally measured data such that the coherence and condition number related observations are validated. Then, a comparison of response predictions as a result of performing Transfer Path Analysis using the matrix inversion technique with different matrix arrangements, all of which are based on coherence knowledge and cross coupling omission is presented. Finally, a new method of improving the quality of the matrix inversion procedure and lowering the condition number of the matrix by selective omission of the cross-coupling terms is presented. It will be shown that the results of the new method are better compared to those of the Moore-Penrose pseudo-inverse technique also having the benefit of not dealing with selection of the singular value rejection threshold.

Keywords: transfer path analysis, TPA toolbox, force identification, matrix-inversion method, pseudo-inversion, cross-coupling omission, condition number

ACKNOWLEDGEMENTS

I would like to express the deepest appreciation to my supervisor Assoc. Prof. Ipek Başdoğan for all the help and support I received during the whole master program. Without her help I would not have been in Koc University enjoying these two very important years of my life. I had the chance to be a part of the Santez project only because of her and this has helped me tremendously in my research and in shaping my future. Her kindness and view over research as a whole have provided the best incentive for work and study and also have allowed me to enjoy both the time spent in the laboratory as well as my free time.

I thank Dr. Murat Sözer and Dr. Kenan Şanlıtürk for their thorough review of my work. I also thank Dr. Polat Şendur from Ford Otosan and Dr. Haluk Erol from Istanbul Technical University for their valuable support during the period of SANTEZ Project.

I thank my project partner Hakan Yenerer for being the perfect work partner and a great and valuable friend. Without his help I would have never reached as far as I am now. He has kept my motivation up all the time not only in the work environment but in all the aspects of my daily life.

I thank my housemate, lab-mate and one of my best friends – Buğra Bayık for always being near me in good and bad days from morning to evening. He made me feel like home in a foreign country and made every single day a day that I want to be happy.

I would also want to thank all my other lab-mates: Utku Boz, Amir Reza Aghakhani, Mustafa Uğur Aridoğan, Murat Gözüm, Hakan Uçar, Egemen Așkin and Gökhan Serhat for being there for me and supporting me throughout my master period.

Last but not least, I thank my wife and family for making everything possible outside my work life and for helping me give life to my dreams. They are the reason for what I am and for where and what I am going to be.

TABLE OF CONTENTS

ABSTRACT iii
ACKNOWLEDGEMENTS v
TABLE OF CONTENTS vi
LIST OF FIGURES ix
LIST OF TABLES xi
CHAPTER 1 1
INTRODUCTION 1
1.1 Overview 1
1.2 Transfer Path Analysis 2
1.2.1 Description of Transfer Path Analysis 2
1.2.2 Uses of Transfer Path Analysis 4
1.2.3 Different approaches to Transfer Path Analysis 5
1.3 Contribution of this Thesis 7
1.4 Outline of the Thesis 8
CHAPTER 2 9
TRANSFER PATH ANALYSIS PERFORMED ON A TRUCK 9
2.1 Introduction 9
2.2 Transfer Path Analysis Theory 10
2.2.1 Restrictions and assumptions 11
2.2.2 Response prediction 11
2.2.3 Path Contribution 12
2.2.4 Force Identification 12
2.2.4.1 Direct measurement of the forces 13
2.2.4.2 Mount Stiffness Method 13
2.2.4.3 Matrix Inversion Method 14

2.3 Description of the Experimental Setup 16
2.4 Instrumentation and Vehicle Preparation 18
2.5 Measurements 20
2.5.1 Frequency Response Measurements 20
2.5.1.1 Quality of FRF and NTF measurements 20
2.5.2 Operational Data Measurement 27
2.6 Results 27
2.6.1 Force Identification 27
2.6.1.1 The Condition Number 30
2.6.1.2 Cabin and engine mount forces 31
2.6.2 Response Prediction 34
2.6.3 Path Contribution 40
CHAPTER 3 43
A NOVEL FORCE IDENTIFICATION APPROACH FOR TRANSFER PATH ANALYSIS THROUGH CROSS-COUPLING OMISSION 43
3.1 Introduction 43
3.2 Improving Response Predictions with Different Matrix Rearrangements: .. 44
3.3 New approach to reducing condition numbers and over-estimation of forces 50
3.3.1 The Moore-Penrose pseudo-inverse 51
3.3.2 The cross-coupling omission method 52
3.3.2.1 Comparison of the three algorithms 55
3.3.3 Comparison of Moore-Penrose Pseudo-inverse and Cross-coupling Omission Method 59
CHAPTER 4 63
DISCUSSION & CONCLUSION 63
BIBLIOGRAPHY 66
APPENDIX 70
TRANSFER PATH ANALYSIS MATLAB TOOLBOX 70
A.1 Introduction 70

A.2 Requirements 70
A.3 Software main interface 70
A.4 Importing Data 72
A.5 Inspecting the imported data 73
A.5.1 Inspected data – plot examples 76
A.6 Running an Analysis 79
A.7 Other Options 81

LIST OF FIGURES

Figure 1: Transfer path analysis quantifies and visualizes the strengths of selected sources and their contribution via multiple transmission paths to a selected receiver signal [*] 3
Figure 2: TPA - One source, two transmission paths and one receiver 10
Figure 3: Source and receiver cabin structure for a typical heavy duty truck 16
Figure 4: Schematic of the vibro-acoustic transfer paths from engine to the receiver and summary of the required data for the analysis 17
Figure 5: Positioning of the tri-axial accelerometer on the rear right cabin suspension at the passive side. 18
Figure 6: Positioning of the microphones on the driver and passenger seats 19
Figure 7: Locations where the measurements were taken 19
Figure 8: Cabin mount - Cabin mount FRF average coherence 21
Figure 9: Engine mount - Engine mount FRF average coherence 21
Figure 10:Cabin mount - Steering Wheel FRF average coherence 22
Figure 11: Engine mount - Steering Wheel FRF average coherence 22
Figure 12:Cabin mount - Mircrophones NTF average coherence 22
Figure 13: Engine mount - Microphones NTF average coherence 22
Figure 14: Frequency domain averaged coherence for cabin FRFs and NTFs 24
Figure 15: Frequency domain averaged coherence for engine FRFs and NTFs 25
Figure 16: Front Right-X to Rear Right-X FRF and Rear Right-X to Front Right-X FRF. 26
Figure 17: Cabin TPA schematic 28
Figure 18: Engine TPA schematic 28
Figure 19: Selection of FRFs for the matrix inversion process 29
Figure 20: Cabin TPA - condition numbers... 31

Figure 21: Engine TPA - condition numbers 31
Figure 22: Cabin forces at engine IDLE condition 32
Figure 23: Cabin forces in 10th gear WOT running condition 32
Figure 24: Engine forces in engine IDLE condition 33
Figure 25: Engine forces in the 10th gear WOT running condition 34
Figure 26: Steering Wheel-Z acceleration during IDLE condition (Cabin TPA) 35
Figure 27: SPL at Front Left Outer Ear (Driver's left ear) during IDLE condition (Cabin TPA) 36
Figure 28: Steering Wheel-Z acceleration during 10th gear WOT condition (Cabin TPA) 36
Figure 29: SPL at Front Left Outer Ear (Driver's Left Ear) during 10th gear WOT condition (Cabin TPA) 37
Figure 30: Steering Wheel-Z acceleration during IDLE condition (Engine TPA) 38
Figure 31: SPL for Front Left Outer Ear (Driver's Left Ear) during IDLE condition (Engine TPA) 38
Figure 32: Steering Wheel-Z acceleration during 10th gear WOT running condition (Engine TPA) 39
Figure 33: SPL at Front Left Outer Ear (Driver's Left Ear) during 10th gear WOT running condition (Engine TPA) 39
Figure 34: Path contribution for the (cabin TPA) predicted acceleration level on the steering wheel in Y direction 41
Figure 35: Path contribution for the (cabin TPA) predicted sound pressure level at the driver’s right ear during the high gear WOT run-up 42
Figure 36: Comparison of Method 2 – direct inverse & pseudo-inverse prediction and measured response at Steering Wheel – Z in IDLE condition 49
Figure 37: Comparison of Method 5 & 6 prediction and measured response at Steering Wheel – Z in IDLE condition 49

Figure 38: Comparison of Method 2,3 & 4 predictions and measured response................. 50
Figure 39: Original condition number of the accelerance matrix 55
Figure 40: Condition number reached with the three algorithms 56
Figure 41: Pairs of cross-couplings removed from the accelerance matrix in order to obtain condition number value of 10 57
Figure 42: Comparison of predictions from the three algorithms 58
Figure 43: Comparison of response prediction at Steering Wheel Z in engine IDLE condition for the pseudo-inverse and new method when condition number is limited to 50 59
Figure 44: Comparison of response prediction at Steering Wheel Z in engine IDLE condition for the pseudo-inverse and new method when condition number is limited to 30 60
Figure 45: Comparison of response prediction at Steering Wheel Z in engine IDLE condition for the pseudo-inverse and new method when condition number is limited to 10 60
Figure A 1: TPA Software Main Interface……………………………………………... 71
Figure A 2: Interface at Startup 72
Figure A 3: Data inspection interface 73
Figure A 4: b) menu when "Inspect FRFs" was selected at point a) 74
Figure A 5:b) menu when "Inspect Operation Data" was selected at point a) 74
Figure A 6: c) menu depending on the type of data inspected 75
Figure A 7: d) menu depending on the type of data imported 75
Figure A 8: View Coherence Metric Button... 75
Figure A 9: Simple FRF plot 76
Figure A 10: A-to-B and B-to-A FRF symmetry verification 77
Figure A 11: FRF coherence Plot 77

Figure A 12: Coherence Metric Plot 78
Figure A 13: Operational Data Plot 78
Figure A 14: Octave band plot for Sound Pressure Level 79
Figure A 15: Main interface after importing data 79
Figure A 16: Main interface after displaying the results 81
Figure A 17: Predicted forces display interface 82
Figure A 18: Example for identifying if a high peak is caused by transfer function or high force 83
Figure A 19: Detailed Contribution Plot 84

LIST OF TABLES

Table 1: Ratio between the predicted and measured RMS values when predicting the response at Steering Wheel-Z for the IDLE condition with the pseudo-inverse 47

Table 2: Ratio between the predicted and measured RMS values when predicting the response at Steering Wheel-Z for the IDLE condition with the direct inversion 47

Table 3: Ratios between the predicted and measured RMS values when predicting the response at Steering Wheel-Z for the IDLE condition with the pseudo-inverse and new method 61

CHAPTER 1

INTRODUCTION

1.1 Overview

Reducing vibration and noise levels inside the vehicle cabin for improving passenger comfort is a key requirement for the automotive industry. Together with stricter legislation requirements, automotive companies are continuously looking for new methods for improvements in this field. In order to meet this objective, engineers work on identifying the possible Noise, Vibration and Harshness (NVH) problems starting from the early stages of vehicle development cycle [1,2].

Transfer Path Analysis (TPA) is a test-based and/or simulation-based procedure that allows tracing the flow of vibro-acoustic energy from a source, through a set of known structure and air-borne transfer pathways, to a given receiver location. TPA follows to evaluate the contribution of the various paths from the source to the receiver, so that the engineers can identify the components along that specific path which need to be modified in order to solve a specific problem.

Performing transfer path analysis is an important step in the vehicle development cycle because it offers insights on the noise and vibration problems which lead to faster troubleshooting, better product development and a systematic approach for the improvement of the vibro-acoustic design. Transfer Path Analysis represents the first step for improving the NVH performance of a vehicle. It consists of identifying the critical paths that transfer the vibration and/or acoustic energy. Once these paths are identified structural modal analysis and/or panel contribution analysis can be performed in order to find the causes of noise and vibration problems.

Transfer Path Analysis can be used to solve vibro-acoustic problems in many applications in addition to automotive industry. Currently, TPA methods are also applied successfully to printers to reduce sound pressure levels, as well as to washing machines or refrigerators. TPA is a systematic method that can be used for all types of structures, large or small, such as cars and ships, or even full aircrafts [1-14].

1.2 Transfer Path Analysis

1.2.1 Description of Transfer Path Analysis

In large structures with multiple sub-assemblies (an automobile, aircraft or ship) the vibro-acoustic sensations are felt by an observer at a location that can be different than that of the source of the vibration. For example, the energy from the engine or wheels of a car is transmitted into the passenger compartment by a number of different paths: from the engine mounts, the exhaust system connection points or the wheel suspension system, etc. Some of the paths are important while some are not. Some of the transfer paths can cause interference at certain frequencies such that the observer does not notice anything significant until he/she changes his/her position. Transfer path analysis is used to assess the structure and airborne energy paths between excitation sources and receiver locations (see Figure 1).

Transfer path analysis is a systematic method that helps the user to understand the relation between multiple sources of noise and vibration and their effect on the user's comfort and health. Transfer path analysis creates a mathematical model of the structure undergoing testing that allows [15]:

- Quantification of the source power
- Ranking of contributions of the different sources along the different paths for all the target receiver positions
- Simulation of what-if scenarios by modifying some of the design variables (eg: changing the stiffness of the connections, etc)

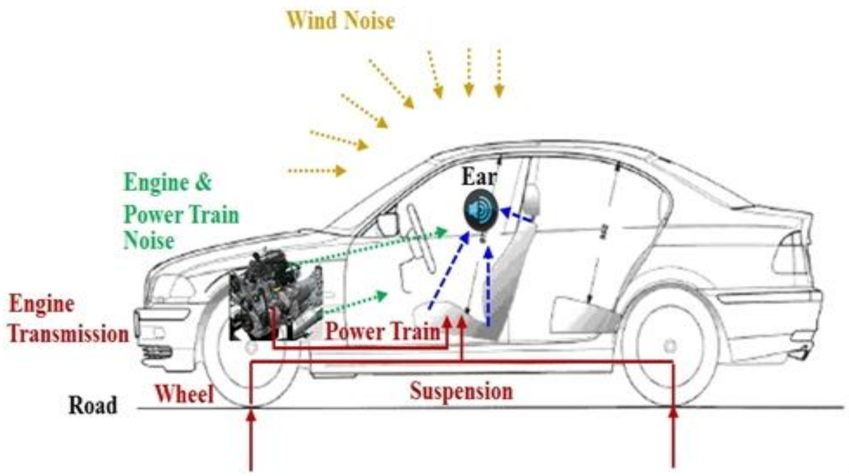

Figure 1: Transfer path analysis quantifies and visualizes the strengths of selected sources and their contribution via multiple transmission paths to a selected receiver signal [*]

TPA allows quantifying the contributions of the various sources and their paths by examining which source is important and which is not, what are the paths that contribute and which of these paths have a cancelling effect. TPA is then used to assess the structure-borne and airborne energy transfer paths from the source of excitation to a given receiver location. After the mathematical model has been created by quantifying the sources and paths, the problems can be identified and engineers can focus on redesigning and improving the system. Typically in the automotive industry, modifications are done on the suspension elements, other body parts or specific body elements that suffer from local impedance changes.

* Figure taken from www.acoustics.org

1.2.2 Uses of Transfer Path Analysis

Transfer path analysis is a powerful tool that can be applied at different stages of a vehicle or a machine development [15].

- ***Troubleshooting***

Sometimes, late in the development process, problems can appear when exchanging major components with others. An example can be given from the automotive sector where the same model of the car can be equipped with different engines: when using a 1.4 liter engine no problems are noticed but when the 2.0 liter engine is equipped, major booming noises appear. If the preliminary examinations point to a structure-borne problem, TPA is used to identify the most effective locations that should be modified. In such case softer/stiffer engine mounts can be used rather than doing major structural redesign.

- ***NVH Refinement***

The targeted sound pressure levels for vehicles interior noise have been considerably lowered during the years. The main noise sources in vehicles are controlled better and better as years pass - engines, drive-train, suspensions. Due to the competition in the industry to improve acoustic comfort, engineers have also directed their attention to other noise contributing sources. These secondary sources can either transmit the energy trough structure-borne paths (gear meshing, engine compartment vibration, etc), or through airborne paths (tire noise, intake noise, etc) or a combination of both. The overall noise level is dependent on multiple sources, thus, NVH refinement requires more and more sophisticated strategies for decreasing/removing noise or vibration contributions from these secondary sources.

- ***Design***

Acoustic optimization can be performed with the help of TPA by using either hybrid finite element models or experimental models [1]. In principle, the designer can substitute different components into the various paths and can record the sounds and then listen and compare the effects. Such “virtual prototyping” approaches are mostly used for trend analysis and are not meant to replace the physical prototype stage.

1.2.3 Different approaches to Transfer Path Analysis

Conventional TPA methods are reliable but their application requires large effort with the main problem being the huge measurement time to build the full data model. For this reason, there are many studies in the literature searching for simpler and faster methods to perform TPA. Some of the transfer path analysis methods are listed below.

- ***OPA – Operational Path Analysis***

OPA [16-18] requires only operational measurements of the path references (body-side mount accelerations, pressures close to vibrating surfaces, etc.) and target responses. It is very time-efficient because it does not require any transfer function measurements, but does not allow the user to identify physical loads and has several limitations that lead to false path contributions (such as when a path is omitted). OPA is based on the transmissibility calculation methods and is performed by using a different model in which the target response is defined using operational responses measured at the load locations instead of the loads themselves.

- ***OPAX – Operational Path Analysis with eXogenos inputs***

OPAX [19] is a TPA method for load identification which combines the speed of the operational path method (OPA) and the effectiveness of the conventional TPA methods. The method uses parametric load models that define the operational forces and acoustic loads based on the measured path inputs. The method follows to make simplifications that create a balance between path accuracy and the time required to perform the analysis.

- ***Time-domain TPA***

In general, the classical TPA approach is applied to stationary and run-up noise problems such as engine noise or road noise. In transient NVH problems such as road bumps, engine start-stop, the classical method cannot be applied because the transient or impulsive phenomenas can't be represented correctly in the frequency domain.

Time-domain TPA [4] is a method where the transfer path NTF's are presented as filter. The multiplication of a force with a transfer function in the frequency domain becomes in the time domain, a convolution of a NTF filter with the time series of a load, representing the contribution of that path but in the time domain.

- ***Multi-reference TPA***

Transfer path analysis techniques are not only used for single coherent sources (e.g.: engine noise), but also for multiple partially-correlated sources (e.g.: road-induced noise in a car). When multiple partially-correlated sources are present in a system, multiple reference spectral processing of the operational measurements is required. Classical TPA techniques can be used for a noise contribution analysis only if the multi-source character can be properly described. The multi-reference cross-power measurements cannot be used directly in a transfer path analysis – decomposition techniques of the multi-reference cross-power data are needed first.

1.3 Contribution of this Thesis

In this thesis, a design methodology that employs experimental TPA methods to predict the vibro-acoustic performance of a truck cabin is presented. The analysis tools and the methodology presented provide a systematic and quantitative way to investigate the end-to-end vibro-acoustic performance of such systems, perform TPA, and identify the critical components of the system that degrade the performance. The TPA method is employed in order to predict the sound pressure level inside a prototype heavy duty truck cabin and the vibration level on the steering wheel.

A MATLAB toolbox is developed so that the Transfer Path Analysis is performed faster and easier. It allows measurement input readings from a file and presents several options for inspecting the inputs and other intermediary variables such as forces, condition numbers, etc. Once all of the initial checks are completed, the noise and vibration predictions and contribution of each transfer path can be also calculated using the comments built-in the MATLAB toolbox.

The major contribution of this thesis is presented in Chapter 3 where different methods are compared to improve the current matrix inversion technique for the force identification process required for TPA. By using measurements of a heavy duty truck, response predictions obtained with the new methods are compared to both the experimentally measured responses and the ones predicted with the classical TPA method. While improving the force identification technique, this thesis also focuses on quantifying the effects of cross-coupling terms on the accuracy of the predicted response. Different matrix arrangements containing some or all of the cross-couplings are compared with previously suggested methods of performing TPA with ‘Diagonal Matrix’ or ‘Mount-wise TPA’ [20]. All the predicted results are also compared with the experimentally measured responses such that effect of eliminating the cross-coupling terms can be observed. The final results are also compared with those obtained through Moore-Penrose pseudo-inverse technique with Singular Value Decomposition (SVD) while having an added benefit of not dealing with selection of the singular value rejection threshold with the proposed method.

1.4 Outline of the Thesis

- In chapter 2, the classic TPA method is employed in order to predict the sound pressure level inside a prototype heavy duty truck cabin and the vibration level on the steering wheel.
- In chapter 3, a comparison of response predictions as a result of performing Transfer Path Analysis using the matrix inversion technique with different matrix arrangements, all of which are based on coherence knowledge and cross coupling omission is presented. A new method of improving the quality of the matrix inversion procedure and lowering the condition number of the matrix by selective omission of the cross-coupling terms is also presented. It will be shown that the results of the new method are better compared to those of the Moore-Penrose pseudo-inverse technique also having the benefit of not dealing with selection of the singular value rejection threshold.
- In chapter 4, the discussion and conclusion section of the thesis is presented.
- In the Appendix, the developed TPA MATLAB toolbox is presented and all of the settings and functionalities are described.

CHAPTER 2

TRANSFER PATH ANALYSIS PERFORMED ON A TRUCK

2.1 Introduction

In this chapter, an end-to-end experimental TPA method has been employed to predict the vibro-acoustic performance of a heavy duty truck cabin. The analysis tools and the methodology presented in this chapter provide a systematic and quantitative way to investigate the vibro-acoustic performance of such systems, perform TPA, and identify the critical components of the system that degrade the performance. TPA method is employed in order to predict the sound pressure level inside a prototype heavy duty truck cabin and the vibration level on the steering wheel. For that reason, first operational internal forces are calculated using the matrix inversion method, then these forces are multiplied with the corresponding FRF's to calculate the required vibration and/or noise responses at the predefined locations. All the data required for the TPA is measured experimentally. To validate the predicted results, coherence of the collected data and the condition numbers of FRF matrices are investigated so that the accuracy of the predicted results can be quantified for the frequency band of interest. The TPA also identifies the contribution of each individual path such that problematic paths can be identified. The predictions of the total response are also compared with the experimentally measured noise and vibration data such that the coherence and condition number related observations are validated.

2.2 Transfer Path Analysis Theory

In order to create a TPA model, the system needs to be divided into an active and a passive part. The active side contains the sources and the passive side contains the points where the responses are measured. The loads are defined at the interfaces between the active and passive parts. The Frequency Response Functions (FRFs) or Noise Transfer Functions (NTFs) define the relationship between the loads and receiver points. In this way, the transfer pats are represented by these FRFs / NTFs [6].

A simple application of a Transfer Path Analysis is shown in Fig 2. The source, in this case the engine, excites the body via two transmission paths: the engine mount 1e-1b (engine side and body side of the mount) and the transmission mount 2e-2b. The vibrations coming from the source are transmitted through various panels and generate noise in the car body by coupling with the air inside.

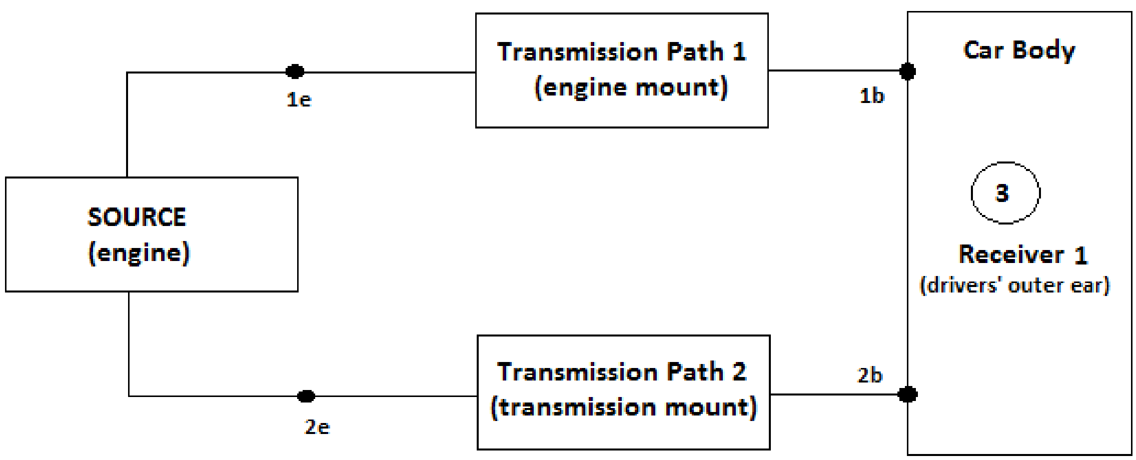

Figure 2: TPA - One source, two transmission paths and one receiver

The aim of the Transfer Path Analysis is to split up the pressure measured at the receiver **(3)** into two partial pressures, caused by the two transmission paths. This is done by separating the system at the connection from the mounts to the body (lb, 2b). If the internal forces acting on the paths are known, then these forces can be multiplied by the Noise Transfer Functions, resulting in the partial pressure from path (1) or (2) to receiver **(3).** Please note that, in most of the Transfer Path Analysis applications, rotations and moments are neglected, only translational displacements and their derivatives (velocity/acceleration) and forces are taken into account.

2.2.1 Restrictions and assumptions

In order to use the traditional formulations of the transfer path analysis, some assumptions and restrictions have to be applied:

- The noise and vibrations have to originate from sources that are coherent (all the measured signals can be related to only one source).
- Only structure-borne noise contributions are examined.
- Only the energy transmitted through the translational degrees of freedom is investigated, the energy transmitted through rotational degrees of freedom are neglected.
- The system is assumed linear and time-invariant in order to apply the superposition principle of the TPA approach

2.2.2 Response prediction

The superposition principle states that the total response at a receiver can be expressed as the sum of its individual path contributions.

The total response (vibration or sound pressure level) is obtained as [6] :

$$rt_j(\omega) = \sum_{i=1}^{N} \frac{r_{ij}(\omega)}{F_i(\omega)} \cdot f_i(\omega) \tag{1}$$

where :

$rt_j(\omega)$: total response (vibration or sound pressure level) at receiver *j* as function of frequency

N : number of transfer paths

$\frac{r_{ij}(\omega)}{F_i(\omega)}$: Frequency Response Function or Noise Transfer Function at receiver *j* due to a force input at transfer path *i*

$f_i(\omega)$: operational force as input to transfer path *i*

2.2.3 Path Contribution

Based on the formulation given for the total response, the individual path contribution to the response at a receiver *j* from a force acting at transfer path *i* is written as [6]:

$$rp_{ji}(\omega) = \frac{r_{ij}(\omega)}{F_i(\omega)} \cdot f_i(\omega) \quad (2)$$

where:

$rp_{ji}(\omega)$: partial response (vibration or sound pressure level) at receiver *j* from a force acting at transfer path *i* as function of frequency

Note: The transfer paths coming from a force acting at a point *i* are examined separately for each of the translational degrees of freedom.

2.2.4 Force Identification

TPA uses the operating forces to calculate the response by multiplying them with the corresponding transfer functions. For that reason, predicting the operational forces accurately is very critical for performing an accurate TPA. Different methods can be employed to identify both structural and acoustics loads. [11,12,32,33]

2.2.4.1 Direct measurement of the forces

Direct measurement of the forces is done by placing force transducers between the engine and the engine mounts. Although it is the most effective method, direct measurement of the loads is not possible in the majority of cases as the load cells require space and well-defined support surfaces, which often makes application impractical or even impossible without modifying the natural mounting. In those cases where direct measurement is possible (i.e. large machinery) it remains the preferred method.

2.2.4.2 Mount Stiffness Method

In case the active and passive structures are connected through flexible mounts, the mount stiffness method can be used. The operational forces can be determined from the complex dynamic stiffness of the mounts $K_i(\omega)$ and of the differential displacement over the mount during operation.

$$F_i(\omega) = K_i(\omega) \cdot \frac{\left(a_{ai}(\omega) - a_{pi}(\omega)\right)}{-\omega^2} \tag{3}$$

where:

$F_i(\omega)$ - mount force

$K_i(\omega)$ - dynamic stiffness of the mount

$a_{ai}(\omega)$ - active side mount acceleration

$a_{pi}(\omega)$ - passive side mount acceleration

When applying the mount stiffness method, it is required to measure the operational displacement both at the source and the receiver side. It is therefore important to place the accelerometers as close as possible to the mount connection. If not measured at the exact location, the measured acceleration signals will not be representative for the problem at higher frequencies. Nevertheless, this method has its limits as accurate mount stiffness data are seldom available and furthermore depend on the excitation amplitude due to their non-linear behavior: modern mounts have a stiffness that changes depending on the operational load on the mount.

2.2.4.3 Matrix Inversion Method

For transfer paths which are represented by rigid connections or where the mount stiffness is very large compared to the body impedance, displacements over the mount are very low, and thus the mount stiffness method cannot be used to identify the load. In these cases, a technique based upon inversion of a measured accelerance matrix between structural response on the receiver side due to force excitation at all transfer paths can be used. If possible, this accelerance matrix should be measured when the source is disconnected from the receiver. This matrix is then combined with operational measurements of the structural vibration at the receiver side in order to obtain force estimates. The matrix inversion method is employed in the case of the heavy duty truck experiment presented in this study due to limited knowledge regarding the mount stiffness. The mounting of the cabin is of a complex nature and its dynamic stiffness cannot be easily determined.

In the matrix inversion method, as the first step, “accelerations” are measured at multiple locations on the support structure during the operating conditions. Typical locations for accelerometer positions are at the passive side of the frame at which the engine mount is connected. In the second step, relation between the interface forces and the motion/deformation is characterized by obtaining the accelerance matrix containing the transfer functions in the frequency domain (FRF). These FRFs from the passive side mount locations to the accelerometer locations are measured in controlled, non-operational conditions.

The forces are obtained as follows [6]:

$$\begin{bmatrix} f_1 \\ \vdots \\ f_n \end{bmatrix} = \begin{bmatrix} \frac{\ddot{x}_{11}}{F_1} & \frac{\ddot{x}_{12}}{F_2} & \cdots & \frac{\ddot{x}_{1n}}{F_n} \\ \vdots & \ddots & & \vdots \\ \frac{\ddot{x}_{m1}}{F_1} & \cdots & \cdots & \frac{\ddot{x}_{mn}}{F_n} \end{bmatrix}^{-1} \begin{bmatrix} \ddot{x}_1 \\ \vdots \\ \ddot{x}_m \end{bmatrix} \tag{4}$$

where:

f_i : the internal operational forces at path *i*

$\frac{\ddot{x}_{ij}}{F_i}$: the local transfer function between the transfer path location i and indicator point j

$\ddot{x}_i$: the operational acceleration at point *i*

m : number of operational accelerations

n : number of forces to be determined

Calculating the inverse of the accelerance matrix in practice can lead to numerical stability issues. It is recommended that the number of measured indicator accelerations should be at least twice the number of forces to be identified (m > 2n). This allows computation of a pseudo-inverse using a least squares estimation of the forces. The condition number of the accelerance matrix is an indicator for the potential amplification of errors. Inaccuracies in the measurement of the FRFs composing the accelerance matrix or in the operational accelerations can lead to large errors in the force estimation if the condition number is high.

Singular value decomposition or other regularization techniques cannot always compensate for the introduced errors. Experimental problems related to impact location and direction and FRF phase accuracy are some of the major factors for high condition numbers. For FRF measurements, reciprocal techniques can be used - exciting at the accelerometer positions. This method saves time and ensures consistency for the recorded data [28].

2.3 Description of the Experimental Setup

Before preparing the vehicle for the experiments, the engineers must determine the significant transfer paths such that the measurements can be performed at those locations. In the case of a heavy-duty truck, one of the goals of the transfer path analysis is to determine the force inputs generated by the engine and to understand the contribution of each of these forces to the overall response at various customer interface points. In this thesis, Transfer Path Analysis was performed to determine the contributions of the paths: a) through the engine mounts, b) through the cabin suspension connections (see Figure 3).

A secondary objective of the transfer path analysis is to determine the overall and partial contribution of each transfer path affecting the comfort of the passengers. Figure 3, illustrates the source and receiver structures for a typical heavy duty truck and the placement of the engine mounts and the cabin suspension connections relative to the chassis.

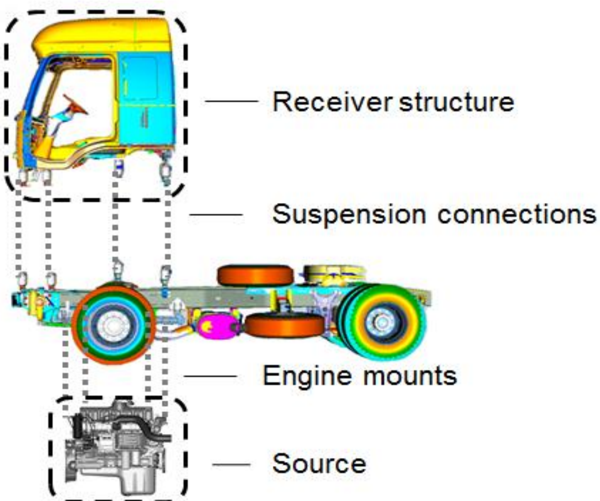

Figure 3: Source and receiver cabin structure for a typical heavy duty truck

To simplify the analysis, transfer paths coming from the exhaust system and other secondary paths were neglected. The transfer path locations include four engine mount locations and four cabin mount locations. Each transfer path is assumed to transmit force in three orthogonal directions. The response points of interest are the steering wheel vibration level and the sound pressure levels at the driver's and passenger's left and right ears.

A schematic of the energy flow from the engine to the cabin is presented in Figure 4. The chart shows that the only paths between the engine and chassis that were analyzed are the engine mounts. Between the chassis and the cabin, the only physical connections are the ones from the cabin suspension system. The arrows represent the measured FRFs and NTFs while the boxes point out the recorded operational accelerations and sound pressure levels.

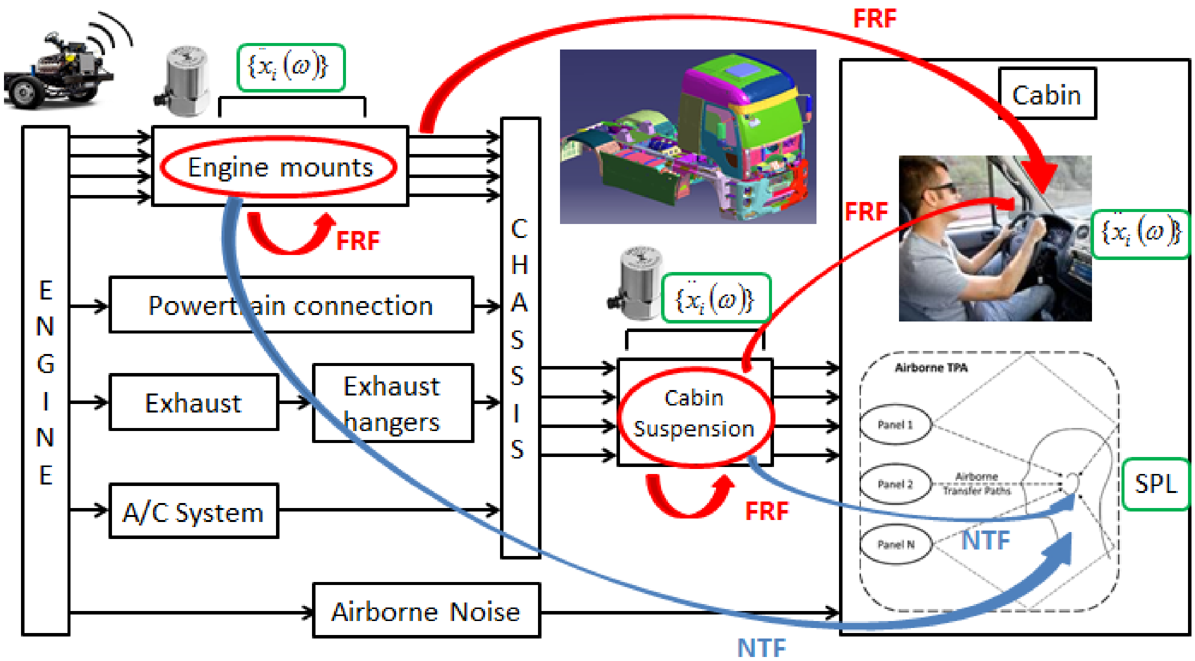

Figure 4: Schematic of the vibro-acoustic transfer paths from engine to the receiver and summary of the required data for the analysis

2.4 Instrumentation and Vehicle Preparation

Tri-axial accelerometers are affixed to the truck frame at the location of the engine mounts at the chassis side, at the passive side of all the four cabin suspension connections and on the steering wheel. Microphones are attached to the seats, close to the position of the driver and passenger left and right ears. As an example, Figures 5 and 6 show the positions of the accelerometers on the rear cabin suspension connections and the microphone locations.

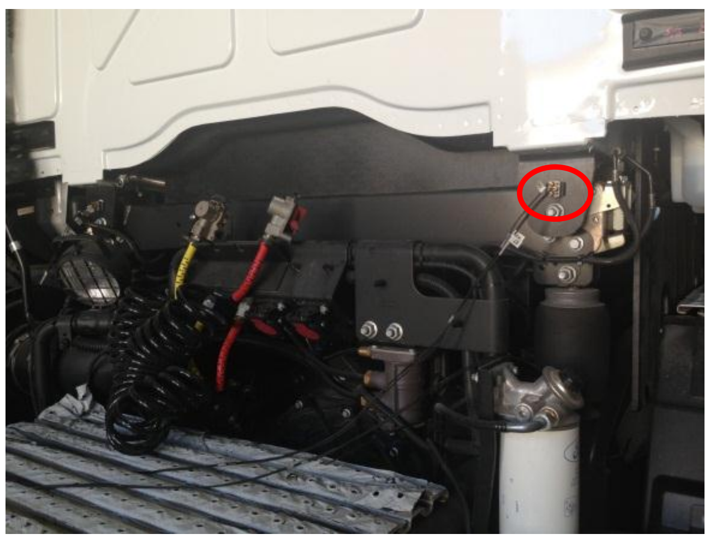

Figure 5: Positioning of the tri-axial accelerometer on the rear right cabin suspension at the passive side.

Figure 6: Positioning of the microphones on the driver and passenger seats

All the FRF and NTF measurements are taken inside a silent enclosed area (Fig. 7A) while the operational measurements are taken on a test track (Fig. 7B).

A) Ford-Gölcük factory B) Ford Eskişehir – Inönü test track

Figure 7: Locations where the measurements were taken

2.5 Measurements

2.5.1 Frequency Response Measurements

FRF measurements are performed using an impact hammer. Firstly, the frequency response functions from the cabin suspension to the microphones and steering wheel are measured. The frequency response functions between the engine mounts themselves and those from the engine mounts to the target response locations are measured afterwards. All the FRF and NTF measurements are taken inside a silent enclosed area as described in the previous subchapter. Impacts are made at each individual path location for each of the three orthogonal directions. The impact hammer tip and the data recording settings for the data acquisition system are selected to obtain the best measurements for a frequency range of up to 200 Hz at a resolution of 0.5 Hz.

2.5.1.1 Quality of FRF and NTF measurements

Transfer Path Analysis is an experiment-based procedure, and for this reason, it is highly dependent on the quality of the measurements. According to Eq. 1, the force identification process depends on the quality of the FRFs between the cabin suspension connections and the operational accelerations at the same locations. The common term for assessing the quality of a FRF measurement is the “Coherence”. The Coherence function (C_{xy}-coherence) between force (x) and acceleration (y) is expressed as:

$$C_{xy} = \frac{|G_{xy}|^2}{G_{xx} \cdot G_{xy}} \tag{5}$$

where:

G_{xy} : Cross spectral density

G_{xx}: Auto spectral density

The coherence function is used as an indication of the quality of the frequency response function measurement and indicates how much of the response energy is correlated to the stimulus energy. If there is another signal present in the response, either from excessive noise or from another signal, the quality of the response measurement is poor. A coherence value of zero for a given frequency indicates no correlation between the response and the stimulus signal. A coherence value of one for a given frequency line indicates that the response energy is 100 percent due to the stimulus signal; in other words, there is no interference at that frequency.

The averaged coherence values of the FRFs for the current experiment are pictured in Figures 8 to 13. All of the FRF and NTF measurements taken from the Cabin mounts have an average coherence of over 90% above the frequency of 20Hz which is a very high value. The positioning of the cabin mounts made the collection of the data much easier than in the case of the engine mounts.

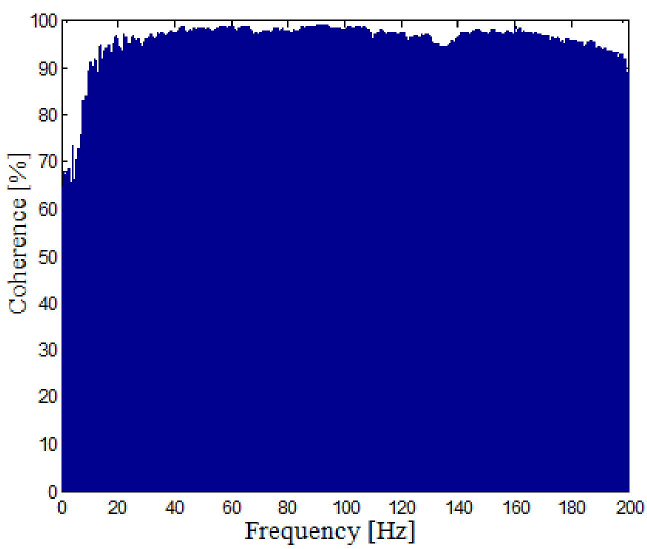

Figure 8: Cabin mount - Cabin mount FRF average coherence

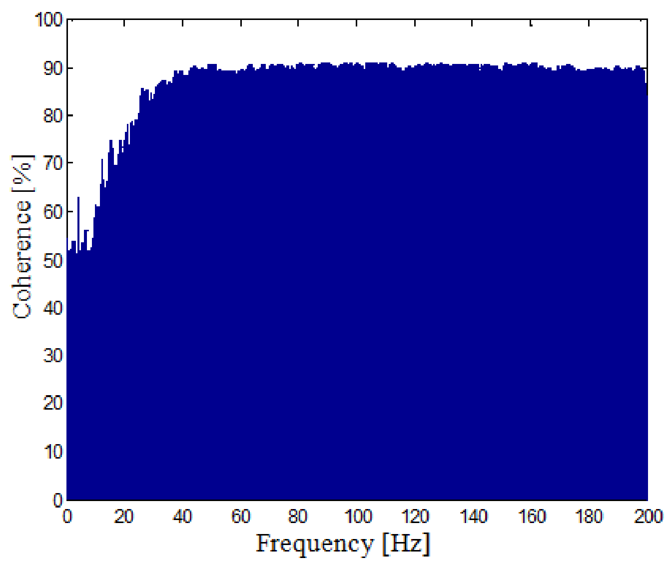

Figure 9: Engine mount - Engine mount FRF average coherence

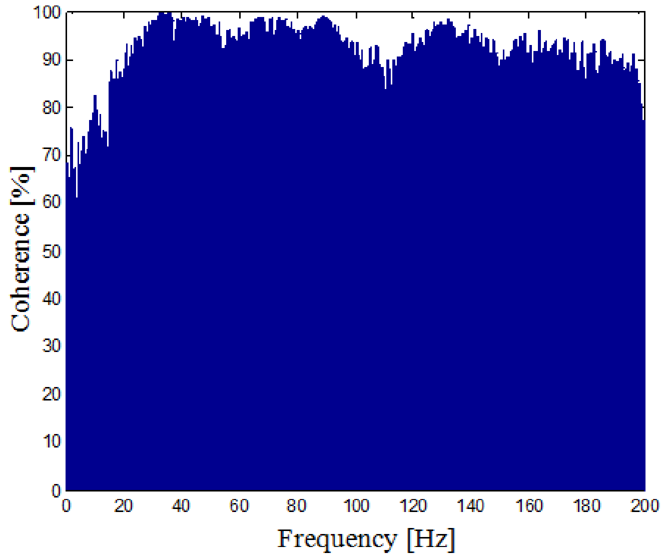

Figure 10:Cabin mount - Steering Wheel FRF average coherence

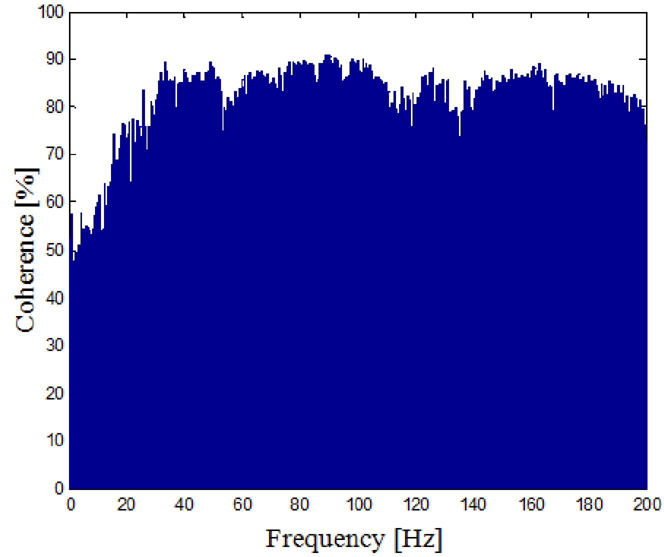

Figure 11: Engine mount - Steering Wheel FRF average coherence

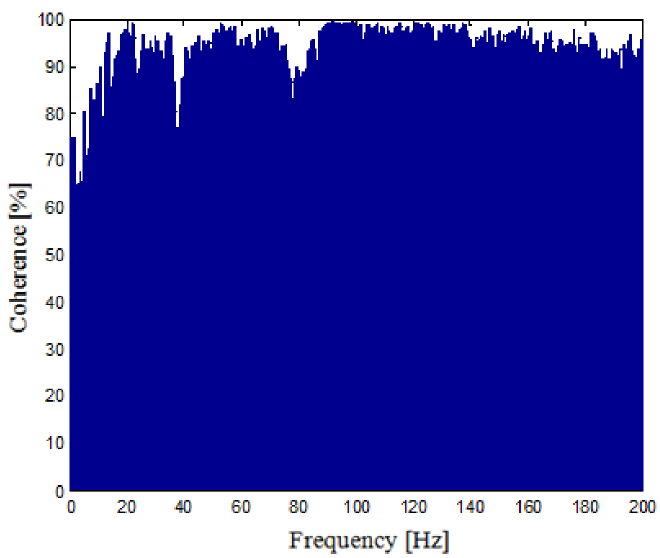

Figure 12:Cabin mount - Mircrophones NTF average coherence

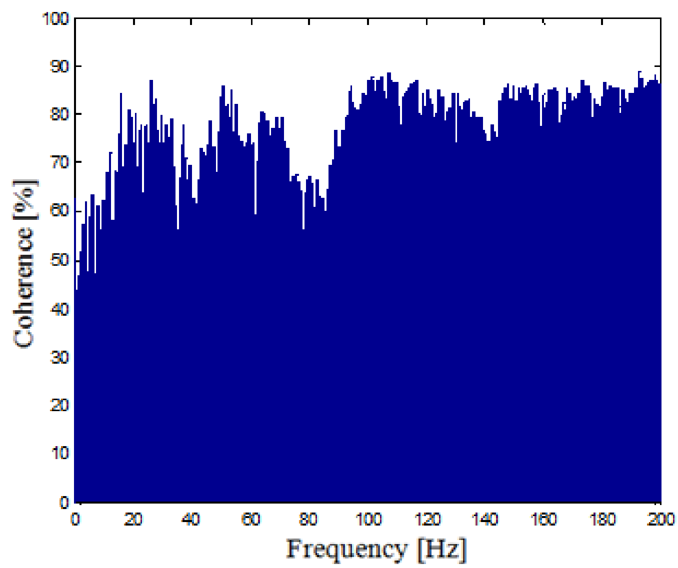

Figure 13: Engine mount - Microphones NTF average coherence

In order to obtain the FRFs and NTFs from the engine, all the hammer impacts were performed under the truck close to the mounts where space was not as available as in the case of the cabin mount hammer impacts. The fact that the engine mounts are further away from the steering wheel and microphones than the cabin mounts has also lead to recording FRFs with a lower coherence (around 85-90% for the engine mounts – engine mounts FRFs and around 80% coherence for the engine mounts – steering wheel FRFs). The NTFs measured from the engine mounts were poor quality, sometimes coherence dropping down even to 60%. NTF measurements could have been recorded better inside an anechoic chamber.

A coherence metric that indicates the individual FRF coherences averaged in the frequency domain was developed to investigate the quality of the measurements. A single element of the matrix represents the averaged frequency of the FRF relating the two locations defined by the name of the row and column on which it belongs to. The nomenclature of the column and row names is described under the figures. The FRFs that are included in the accelerance matrix are found in Figures 14 and 15 at the left of the dotted red line. Above and under the dotted white line, at symmetric positions, are the FRFs relating two different suspension connections. The two FRFs were measured separately by hammer impact by excitation from each side of the mounts. At the right of the dotted red line, the coherences of the FRFs and NTFs that describe the source-receiver relation.

In both figures, the coherence of FRFs to the Steering Wheel-Y is lower than all others. This shows that a sensor problem affected the measurements. In the case of the engine FRF measurements there was an additional problem – from Figure 15 it can be observed that the excitation at the Front Left-X engine mount was not correctly performed thus leading to erroneous recording of the FRFs from that point to all the other locations.

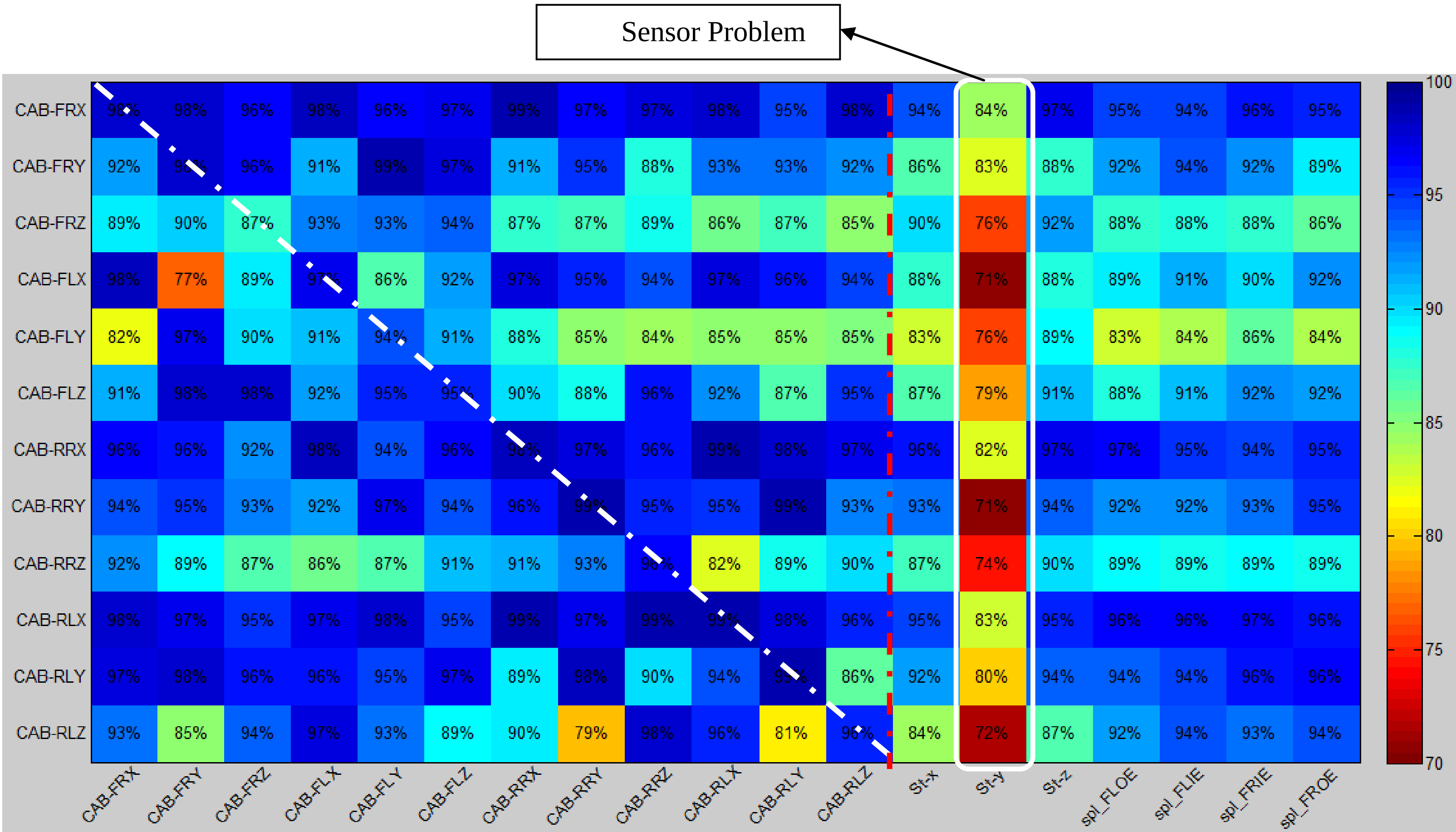

Figure 14: Frequency domain averaged coherence for cabin FRFs and NTFs

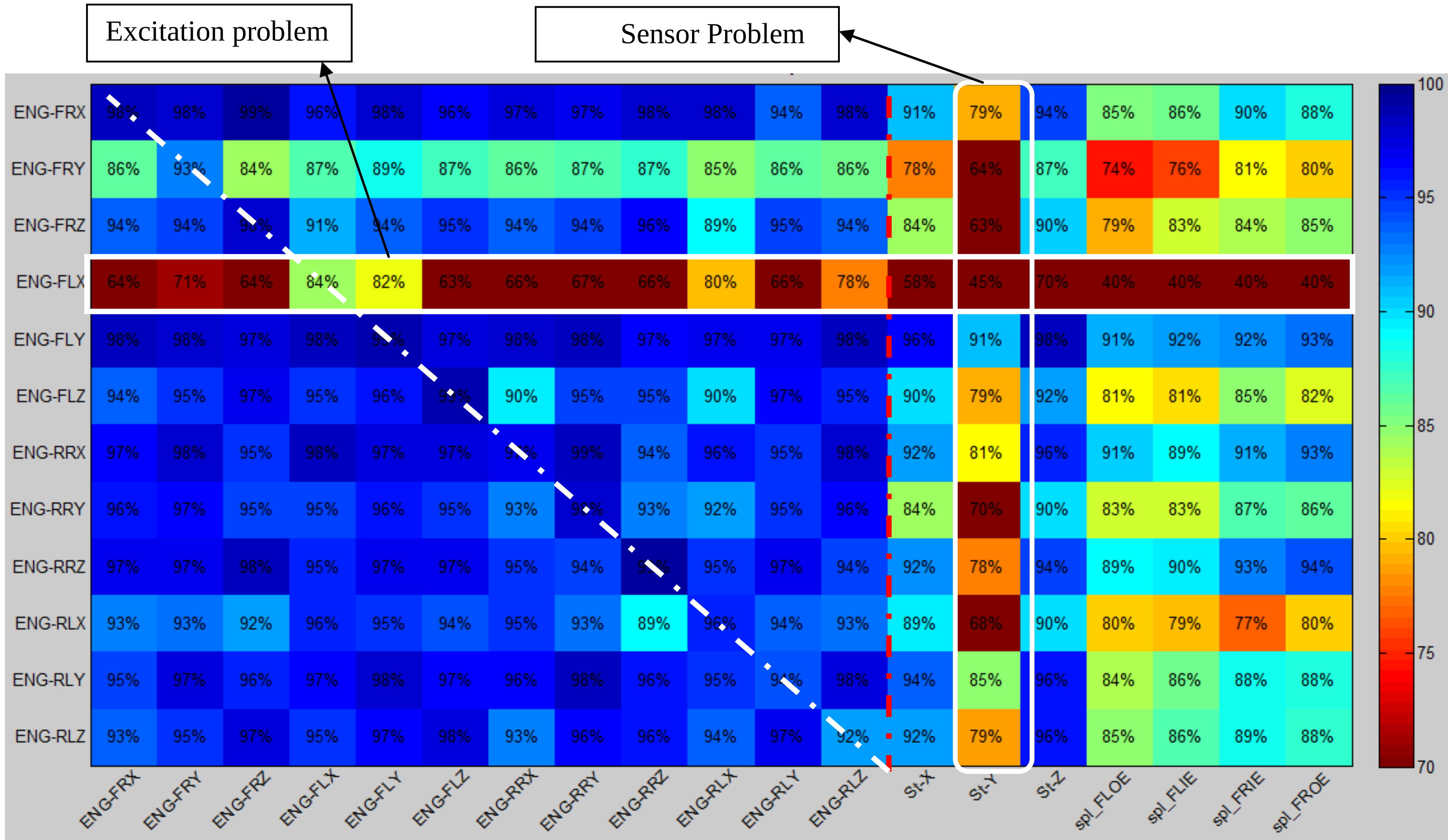

Figure 15: Frequency domain averaged coherence for engine FRFs and NTFs

where:

ENG – Engine CAB – Cabin

FL – Front Left suspension connection

FR – Front Right suspension connection

RL – Rear Left suspension connection

RR – Rear Right suspension connection

St – Steering Wheel

X, Y, Z – The three orthogonal directions

As deducted from the figures above, the hammer impact testing is prone to human errors and cannot be performed in perfect conditions. Perfect FRF measurements are impossible also due to the fact that the impact location cannot occupy the same physical space as the placement location of the sensor. These two major factors are reflected in Figure 16 where two FRFs from symmetric positions on the accelerance matrix have similar average coherence but when plotted on top of each other prove to be different.

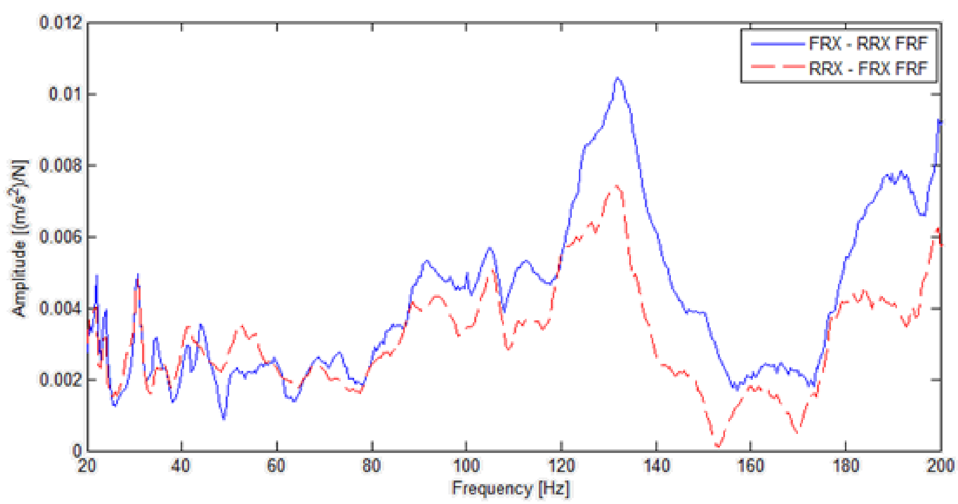

Figure 16: Front Right-X to Rear Right-X FRF and Rear Right-X to Front Right-X FRF

2.5.2 Operational Data Measurement

The operational accelerations and sound pressure levels need to be recorded so that the in-operational internal forces can be determined (see Eq. 4). They are also used to check the accuracy of the predicted result. The measured operational accelerations or sound pressure levels are generally compared with the ones obtained from the transfer path analysis before the path contributions are examined.

For the current setup, the recorded data includes the tri-axial accelerations from each of the engine mounts and cabin suspension connections, and also the recorded outputs from the microphones and the accelerations on the steering wheel.

The experiments were performed for two different operating conditions of the truck. The first set of data is recorded while the truck is stationary with the engine running at idle speed and the second set of data is recorded while the truck is driving on a test track in the 10^{th} gear during a wide-open-throttle (WOT) engine run-up.

The measurements are recorded in time domain over a period of approximately 10 seconds after which the time domain data is converted in frequency domain by taking FFT.

2.6 Results

2.6.1 Force Identification

Two factors influence the response at a certain point (see Eq. 1 and 2). These are the forces acting on the system and the FRFs or NTFs that relate the forces to the response location. In order to see the cause of a high amplitude acceleration or sound pressure level at the target location both of them need to be investigated.

In the current study, the matrix inversion method is used to identify the forces acting on the paths. When the experiment is performed on a system without disassembling the source and the components, the matrix inversion process becomes a direct inversion which results in unique operational forces.

To identify the forces acting on the passive side of the engine mounts, the measured FRF's between the four mounts in each of the three directions form a series of 12x12 square matrices for each frequency. These matrices are inverted (direct inversion) and multiplied with the set of operational accelerations at the mounts to obtain the internal operational forces (see Eq. 4). The same procedure is applied to identify the internal forces acting at the passive side of the cabin suspension connections. When TPA is performed for two different operational conditions (e.g.: operational high gear engine run-up and idle condition), the matrices remain the same. In the force identification process, only the operational accelerations change.

In figures 17 and 18, a schematic of the Transfer Path Analysis measurement locations is presented. The yellow arrows indicate the Cabin-Cabin or Engine-Engine FRFs that will be involved in the matrix inversion process while the red lines indicate the FRFs/NTFs that will relate the operational internal forces acting on the paths to the response locations.

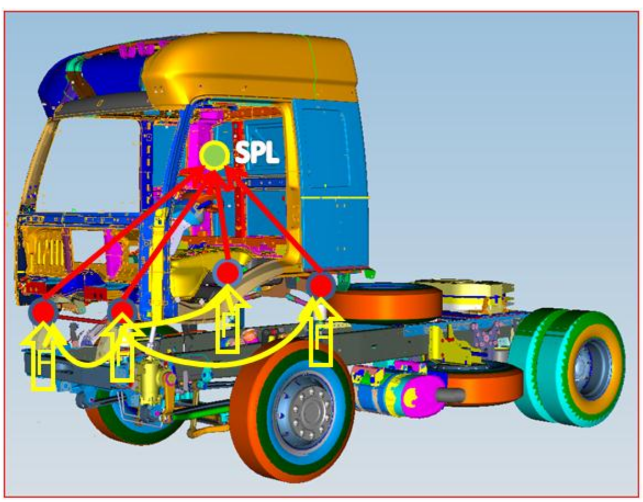

Figure 17: Cabin TPA schematic

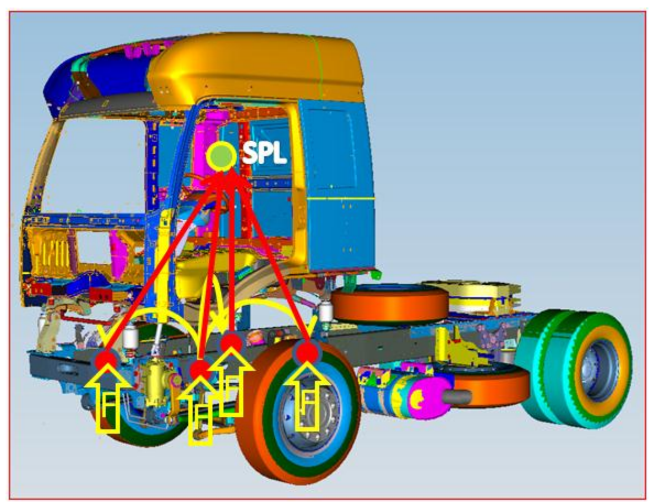

Figure 18: Engine TPA schematic

Based on the Coherence metric presented in the previous chapter, the FRF measurements with the highest coherence value, averaged in the frequency domain are selected to replace their counterparts above or under the diagonal of the accelerance matrix. In this way, the accelerance matrix becomes symmetric. The process is depicted in figure 19.

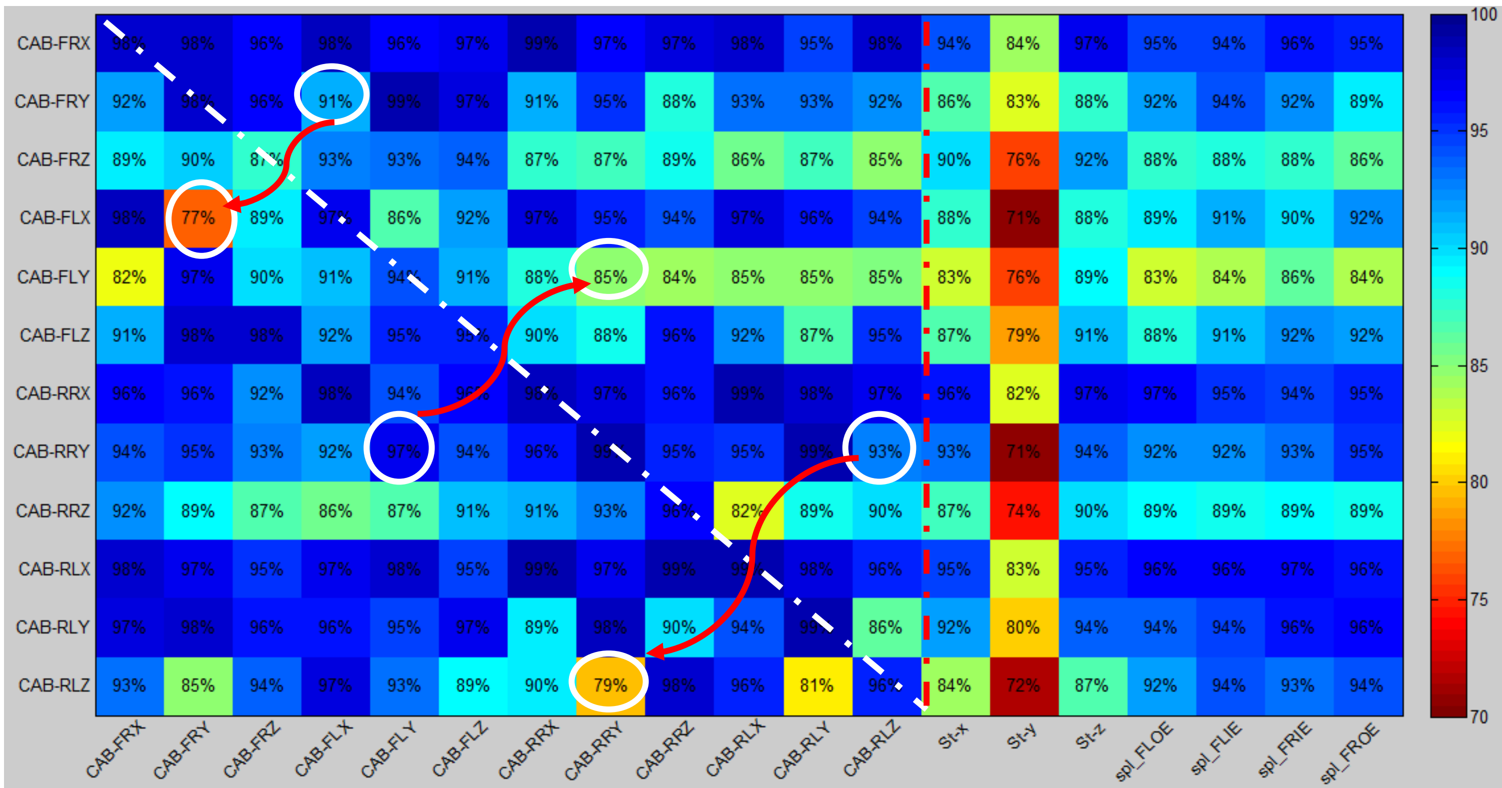

Figure 19: Selection of FRFs for the matrix inversion process

2.6.1.1 The Condition Number

The condition number of a matrix represents the ratio of the largest singular value to the smallest singular value and it is an indicator of the ill-conditioning of the matrix. The high condition numbers may be a consequence of strong modal behavior of the structure. If a small number of modes dominate the behavior of a structure, the responses at the path interfaces are not independent of each other. If many modes contribute to a specific response, the columns of the accelerance matrix will be linearly independent, resulting in a low condition number [21,22]. This way, the condition number can be used as a metric to determine the accuracy of the force identification process. The condition number is a property of a matrix and it is expressed as:

$$cond(A) = \|A\| \cdot \|A^{-1}\| \qquad (6)$$

where $\|A\|$ is the norm of the matrix A.

The condition number shows how accurate the vector *x is* when solving a system of $A \cdot x = b$. If the condition number is close to one, the matrix is called well-conditioned which means the inversion can be computed with good accuracy. If the condition number is high, then the matrix is ill-conditioned. If the measurement errors in matrix A are negligible and the matrix is well conditioned the internal force estimation becomes reliable. High condition numbers of the accelerance matrix often lead to the magnification of small response errors into large force errors.

After selecting the best FRFs for composing the accelerance matrix, the condition numbers for the cabin and engine TPA cases can be obtained. The values for the condition numbers are shown in figures 20 and 21.

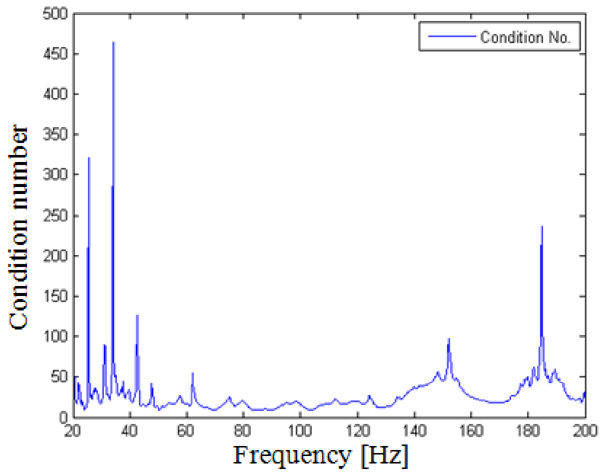

Figure 20: Cabin TPA - condition numbers

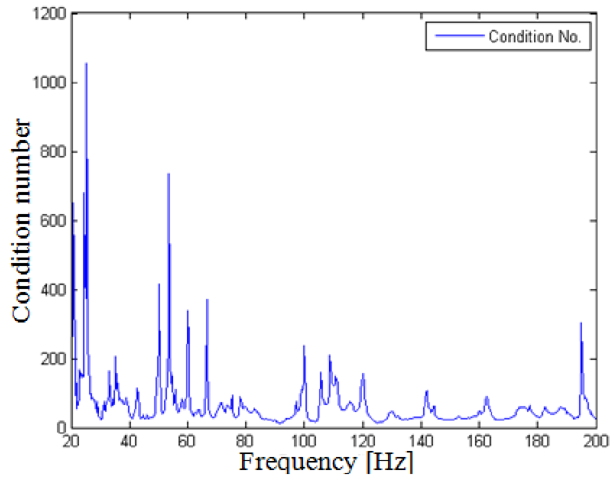

Figure 21: Engine TPA - condition numbers

The condition numbers obtained for the Engine TPA were much higher than in the case of the Cabin TPA. These results were expected since the quality of the measurements taken at the engine mounts was also lower than that of the measurements taken from the cabin. For the cabin condition number, high peaks were noticed under the frequency of 40 Hz reaching values of up to 450. In the frequency range of 140-200 Hz condition numbers were also a little high. For the engine TPA, condition numbers reached values of up to 1000 while the average values are around 50-100 compared to the 25-50 average condition numbers found for the cabin TPA.

2.6.1.2 Cabin and engine mount forces

Different forces act on the cabin and engine mounts depending on the operational conditions (engine IDLE and 10^{th} gear WOT run-up). Figures 22 to 25 show the forces acting on the cabin and engine mounts at both of the operational conditions.

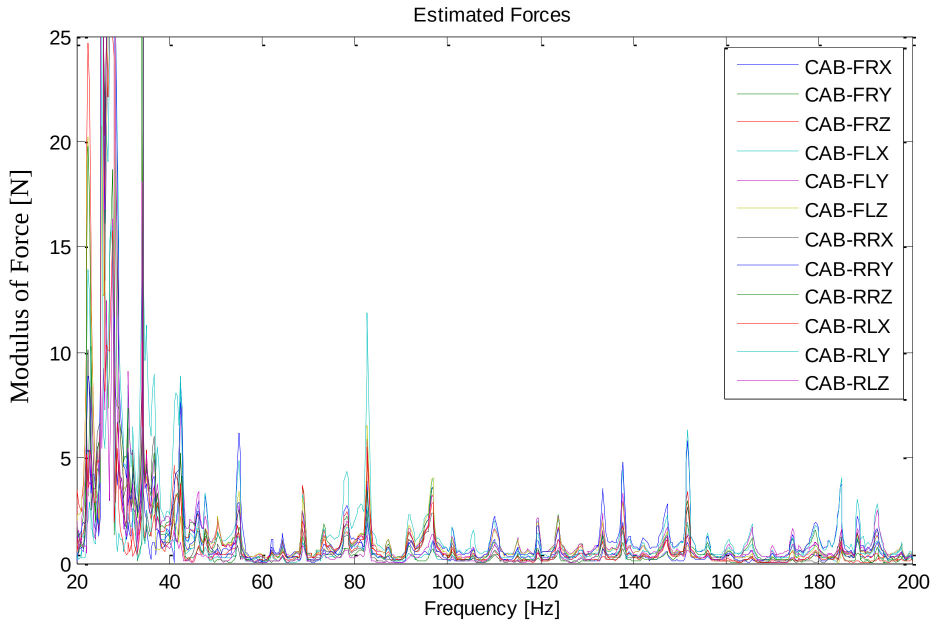

Figure 22: Cabin forces at engine IDLE condition

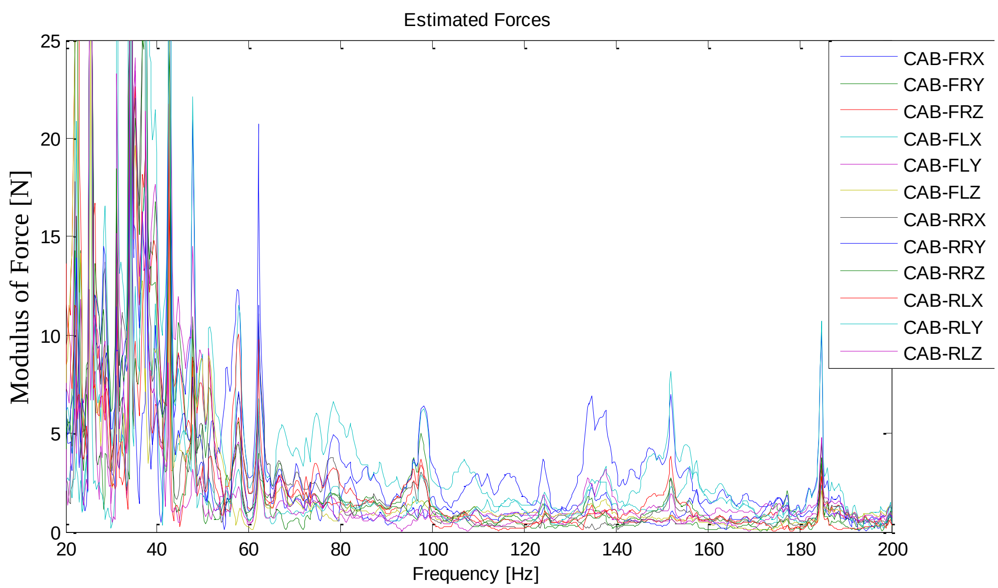

Figure 23: Cabin forces in 10th gear WOT running condition

The high condition numbers for the cabin TPA in the low frequencies caused very high force over-estimations as it can be seen from figures 22 and 23. If the forces estimated in the frequency band of 60-200 Hz were around the values of 0-10 Newton, in the low frequencies they went above 100 Newton because of the high condition numbers. The influence of the ill-conditioning of the accelerance matrix can be noticed in figure 23 also around the frequencies of 150Hz and 180Hz where unexpected peaks in the force have been observed.

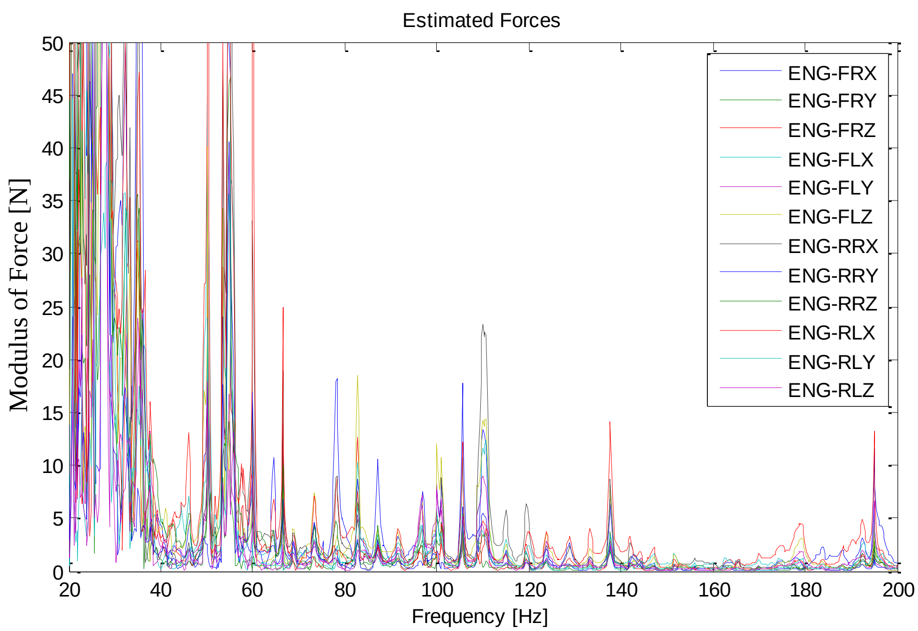

Figure 24: Engine forces in engine IDLE condition

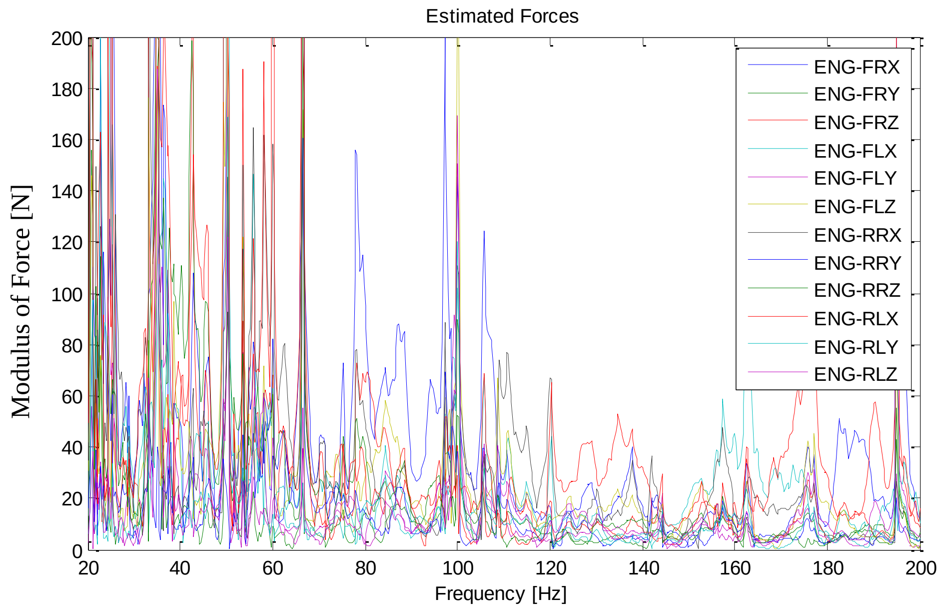

Figure 25: Engine forces in the 10th gear WOT running condition

Same as in the case of cabin forces, the engine forces (Fig. 24 and 25) are highly influenced by the ill-conditioning of the accelerance matrix. Very high over-predictions are noticed at the points where the condition numbers are high. In the frequency bands where the force was not predicted correctly it is expected that the response predictions and path contributions will also be incorrect.

Looking at the other areas of the frequency band, it can be noticed that the forces during the 10^{th} gear WOT running condition are up to 6-7 times higher than those predicted during the IDLE running condition.

2.6.2 Response Prediction

In real life situations, the vibration or sound pressure level at the target point of interest is measured. In transfer path analysis, the response prediction step is mostly regarded as a means of validating the accuracy of the measured data and provides an indicator on how precise the force identification is and how reliable the path contributions will be. A good match between the measured and predicted response is obtained only if the forces were identified correctly and the transfer functions relating the forces to the response target location were measured precisely.

The goal of the Transfer Path Analysis on the truck was to identify the contributors to eventual vibration levels on the steering wheel and high peaks in the sound pressure level at the driver and passenger ear locations. For this reason a total of 7 response locations were selected 3 of which being the tri-axial accelerations on the steering wheel and the other 4 the sound pressure levels at the driver and passenger left and right ears.

In this thesis, response predictions for one of the accelerations on the steering wheel is presented for each of the four situations and four more predictions for the sound pressure level at the driver's left ear. In Figures 26-29 the Steering Wheel-Z acceleration predictions and Front Left Outer Ear SPL predictions are presented for the case of IDLE and 10WOT conditions for the Cabin TPA (see Figure 17 for the description).

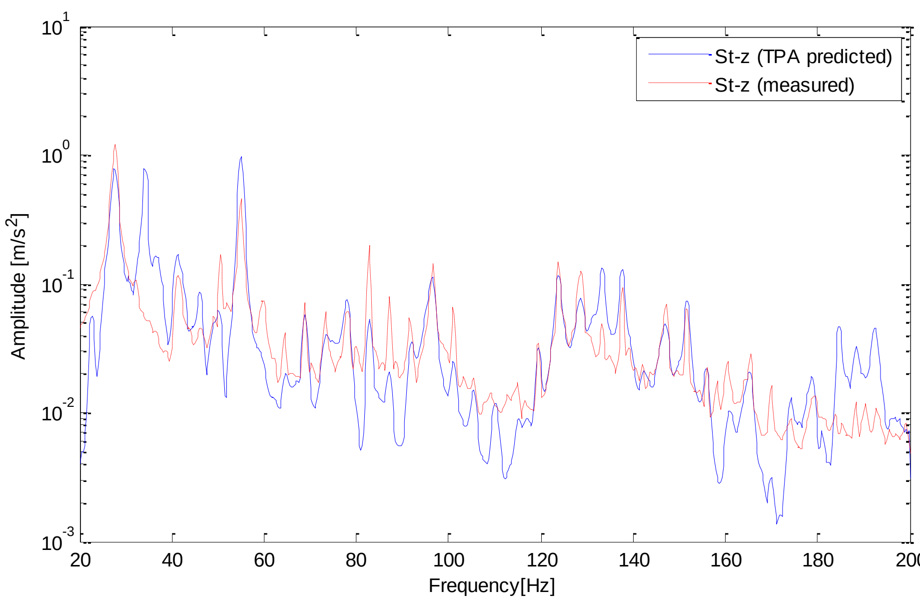

Figure 26: Steering Wheel-Z acceleration during IDLE condition (Cabin TPA)

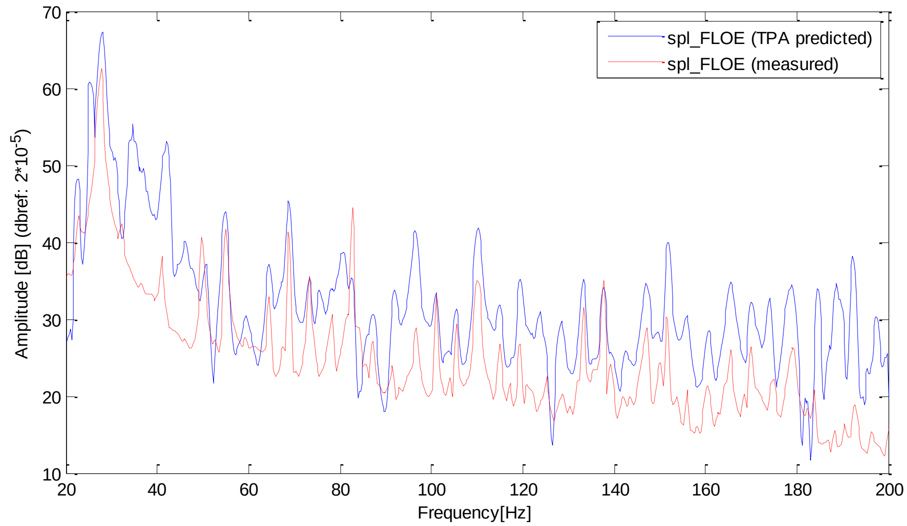

Figure 27: SPL at Front Left Outer Ear (Driver's left ear) during IDLE condition (Cabin TPA)

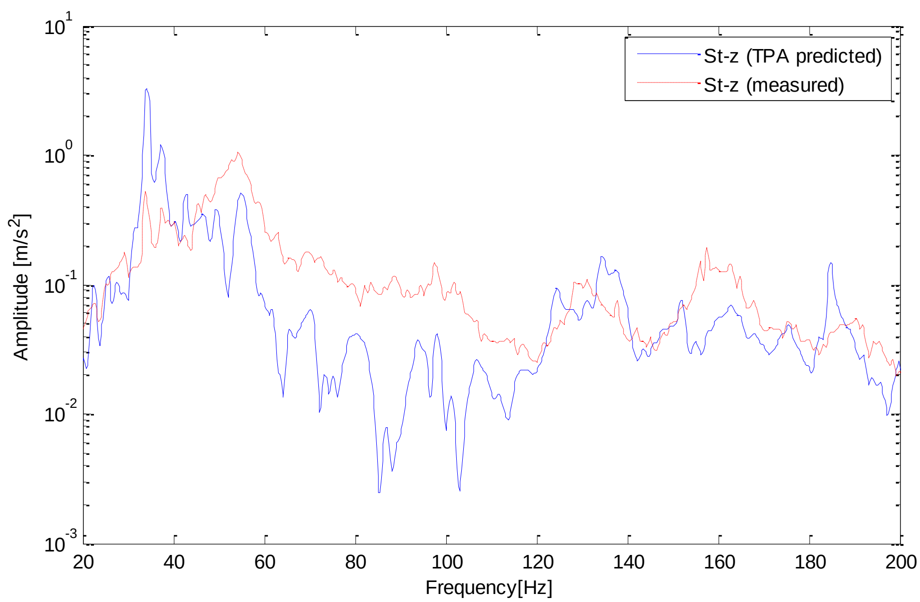

Figure 28: Steering Wheel-Z acceleration during 10th gear WOT condition (Cabin TPA)

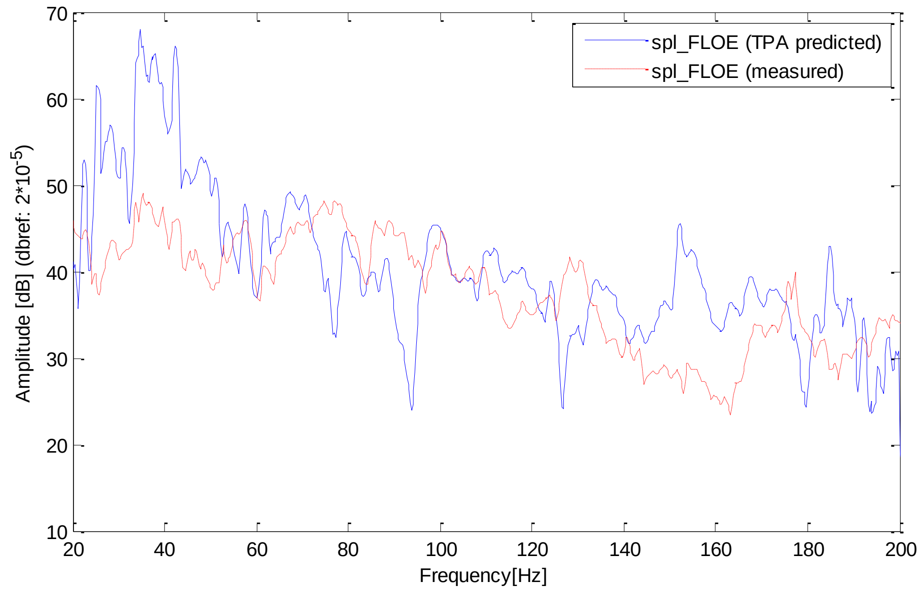

Figure 29: SPL at Front Left Outer Ear (Driver's Left Ear) during 10th gear WOT condition (Cabin TPA)

Good predictions were obtained for both the accelerations and the sound pressure levels for the Cabin TPA during the engine IDLE condition. The best force estimates were obtained in the same conditions which eventually lead to good response predictions. Decent results were also obtained during the 10th gear WOT condition while predicting the acceleration on the steering wheel. Predicting responses for a vehicle running on the track is of course a less reliable process than predicting responses in stationary conditions. During track test measurements, there are a lot of noise disturbances and vibrational paths that remain unaccounted for, thus leading to lower quality predictions. As for the SPL, the results were matching less due to the fact that the NTF measurements were not performed in an anechoic chamber.

In Figures 30-33 the Steering Wheel-Z acceleration predictions and Front Left Outer Ear SPL predictions are presented for the case of IDLE and 10WOT conditions for the Engine TPA (see Figure 18 for the description).

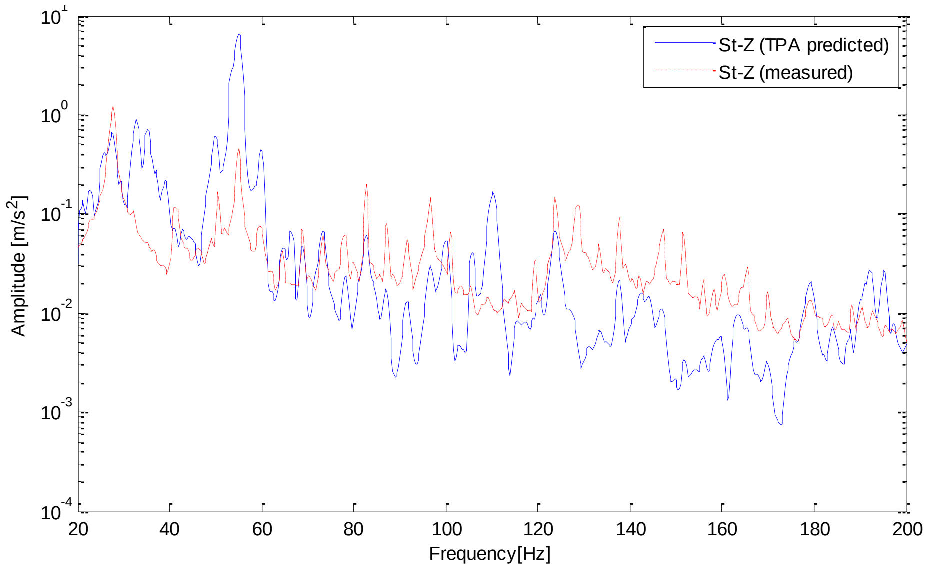

Figure 30: Steering Wheel-Z acceleration during IDLE condition (Engine TPA)

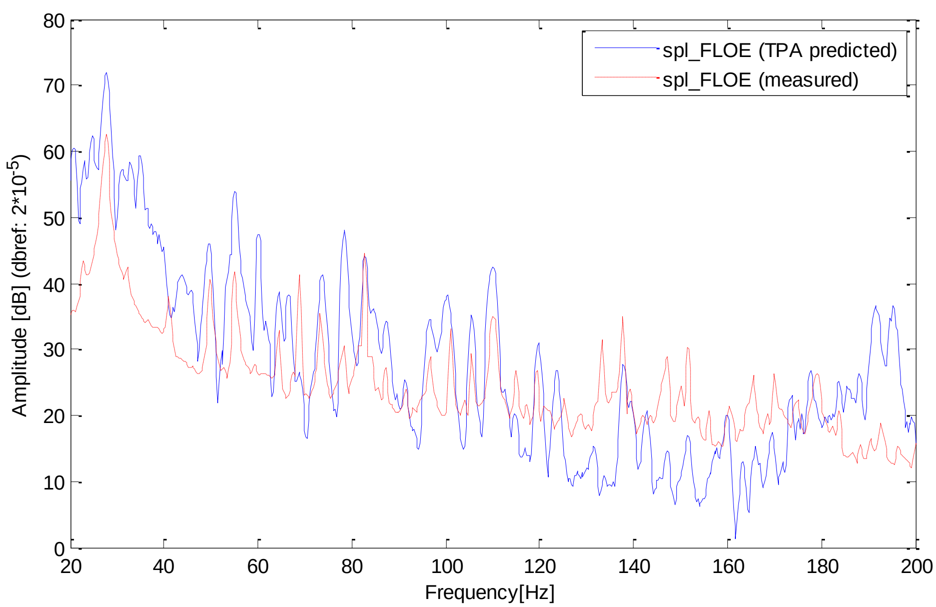

Figure 31: SPL for Front Left Outer Ear (Driver's Left Ear) during IDLE condition (Engine TPA)

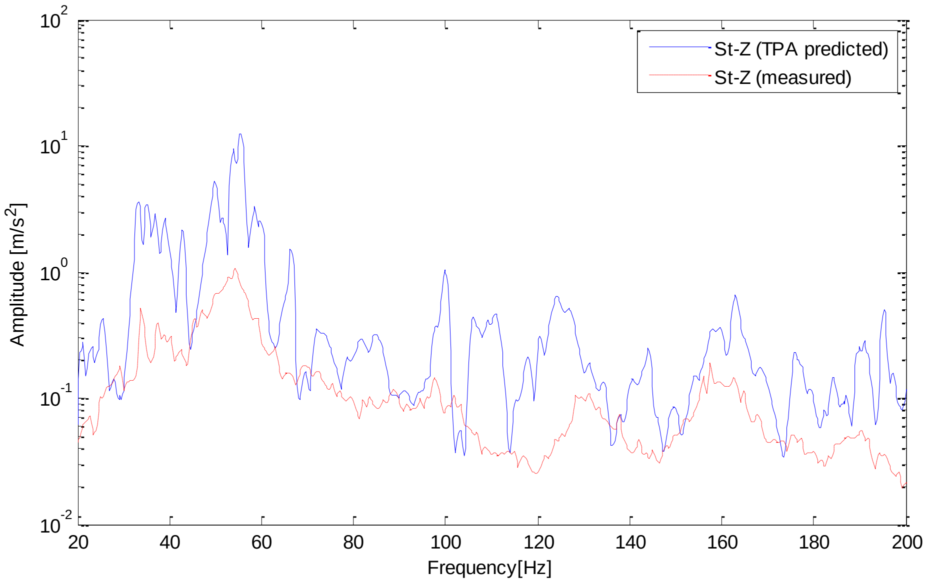

Figure 32: Steering Wheel-Z acceleration during 10th gear WOT running condition (Engine TPA)

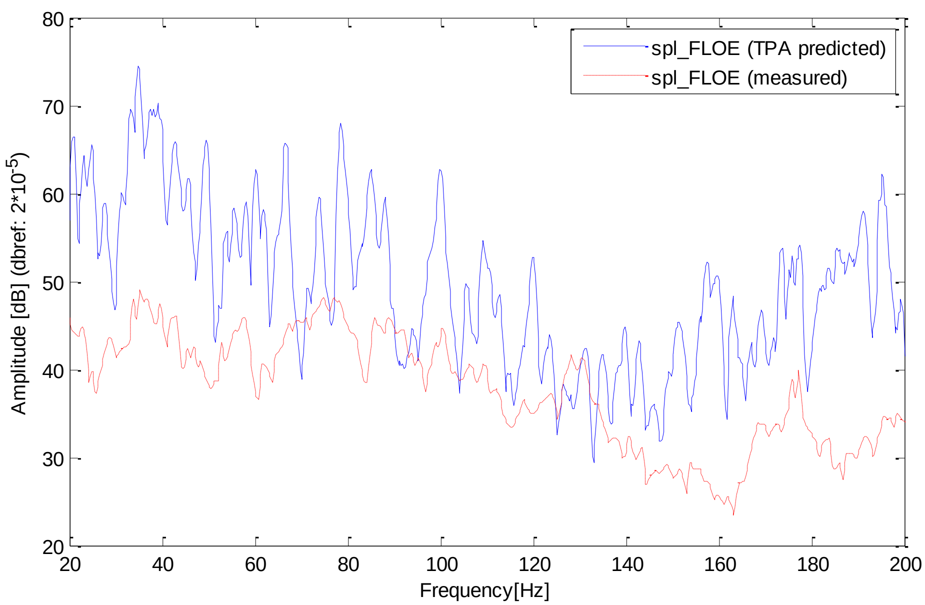

Figure 33: SPL at Front Left Outer Ear (Driver's Left Ear) during 10th gear WOT running condition (Engine TPA)

For all the Engine TPA predictions, the force identification step played a huge role. Since the force estimates were over-predicted in most of the areas of the frequency band, the response predictions were also higher than the measured ones. In the case of the 10^{th} gear WOT running condition for the Engine TPA, the predictions were extremely different than the measured ones because of the added effect of missing paths in the analysis. During the running condition, forces coming from the road through the suspension system, forces acting at the connections of the exhaust system and other auxiliary paths play a much more important role, causing the final results to be very far from the truth.

2.6.3 Path Contribution

Path contribution for a specific response can be correctly identified when the prediction for the target vibration or sound pressure level is also performed with a high level of confidence. The results of a contribution analysis (obtained with Eq. 2) to the receiver can be trusted when the summed contributions from all the paths correspond well to the measured receiver levels. If the two do not match well it can be because of the data quality but it can also be due to the fact that the receiver is affected by other sources or transfer paths which have not been included in the analysis. These can be airborne paths, or in case of road tests, road noise or aerodynamic noise.

Because of the good prediction and low condition numbers in the 60-120 Hz frequency band (Figure 20) the acceleration level on the steering wheel in Y direction is presented in Figure 34 along with its contributors. The cold color region represents the low contribution areas while the hot color region points to high contributions. The most contributing path is the front left cabin suspension connection in the Y direction, which makes sense since the steering wheel position is in the front left side of the cabin and the direction of the investigated response is the Y direction.

In noise and vibration testing the central point of interest is the high amplitude frequency bands. In Figure 34, two main peaks for the acceleration are closely predicted and for both of them, the contribution plot points to the same two major components. Such results are critical in understanding how the energy is transferred through the suspension connections to the steering wheel or other components inside the cabin. The result is just an example that shows the quality of the results obtained during the experiment.

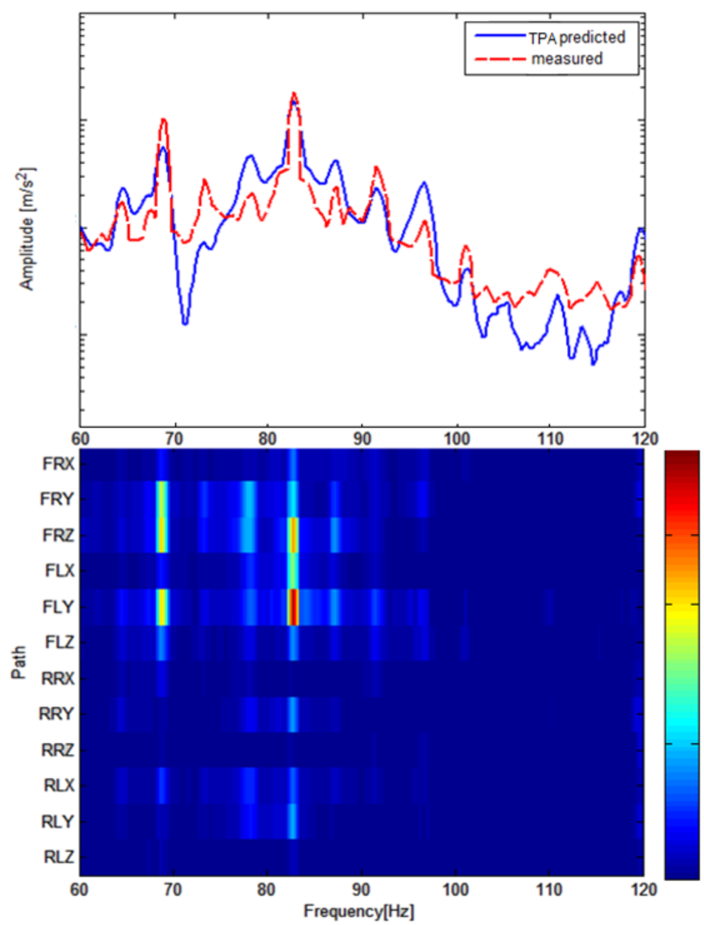

Figure 34: Path contribution for the (cabin TPA) predicted acceleration level on the steering wheel in Y direction

The high SPL identified at the Driver's right ear is depicted in Figure 35 together with the contributions to that response for the 60-120 Hz frequency band where the cabin condition numbers were low. The Z components of the front right and rear left cabin connections are the specific contributors to the noise at 70Hz. If the high contribution is caused by the internal force, then the physical connection of the suspension can be modified to result in a decrease of the sound pressure level. If it is because of the NTF, then in addition to analyzing the component of that specific path, a panel acoustic contribution analysis can be performed and vibrating panels of the cabin can be identified and modified to lower the contribution of these paths.

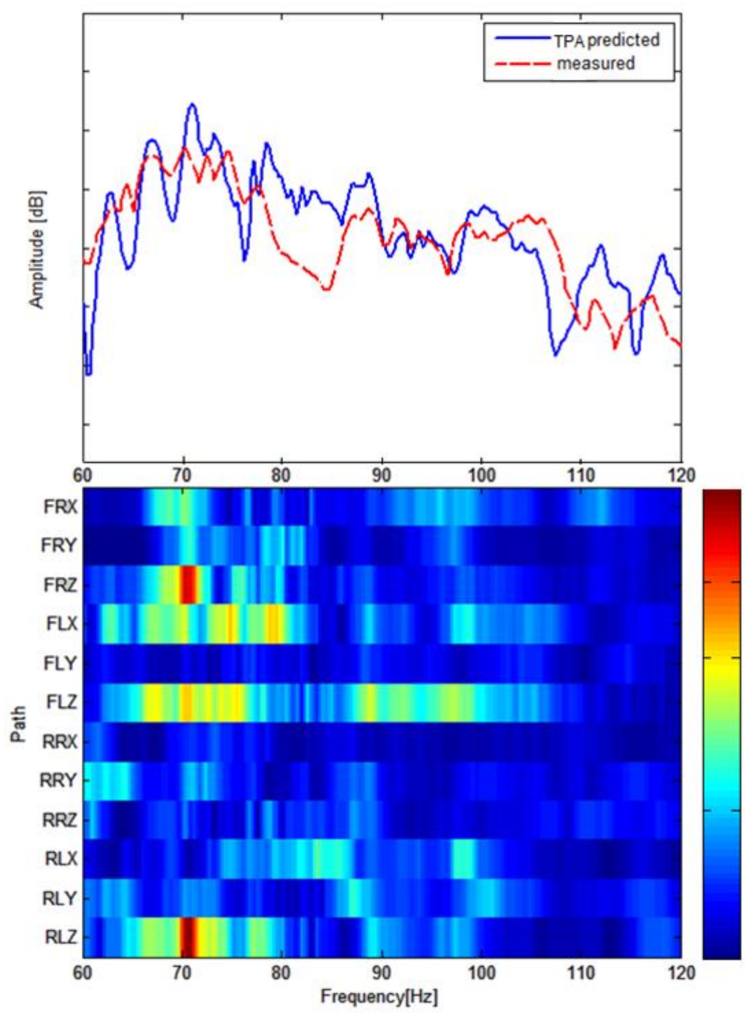

Figure 35: Path contribution for the (cabin TPA) predicted sound pressure level at the driver's right ear during the high gear WOT run-up

CHAPTER 3

A NOVEL FORCE IDENTIFICATION APPROACH FOR TRANSFER PATH ANALYSIS THROUGH CROSS-COUPLING OMISSION

3.1 Introduction

The classical TPA method requires correct determination of the operational forces at the interfaces between the active and passive sides of the structure. Since the path contribution to a response is the product of the internal force and the corresponding transfer function to that specific response, obtaining the real internal forces is critical in doing a reliable path contribution analysis. Direct measurement of the forces using transducers can be difficult and it is rarely performed due to physical limitations. The other option is to obtain the forces indirectly by using the dynamic stiffness method [23, 24] or the matrix inversion method [25, 26]. The dynamic stiffness method is more precise but can be used only when elastic components are present at the interfaces between the active and passive sides and their dynamic stiffness properties are known in advance. The matrix inversion method is used when the transfer paths are very stiff compared to the receiver structure and the relative operational displacement becomes very small. Obtaining the forces requires inverting a matrix of measured FRFs at each frequency. However, errors in the measurement of FRFs and operational responses together with ill conditioning of the FRF matrix at certain frequencies may cause wrong force estimation at those interface locations which also lead to a misleading path contribution analysis [27-29].

This chapter presents different methods to improve the current matrix inversion technique for force identification required for TPA. By using measurements of a heavy duty truck, response predictions obtained with the new methods are compared to both the experimentally measured responses and the ones predicted with the classical TPA method. While improving the force identification technique, this chapter also focuses on quantifying the effects of cross-coupling terms on the accuracy of the predicted response. Different matrix arrangements containing some or all of the cross-couplings are compared with previously suggested methods of performing TPA with 'Diagonal Matrix' or 'Mount-wise TPA' [20]. All the predicted results are also compared with the experimentally measured responses such that effect of eliminating the cross-coupling terms can be observed. It is also observed that the force is over-predicted at the frequencies where the inverted matrix is ill-conditioned. For that reason, the second method presented in this chapter aims reducing the condition number and thus avoiding the over-prediction. The results are also compared with those obtained through Moore-Penrose pseudo-inverse technique with SVD while having an added benefit of not dealing with selection of the singular value rejection threshold with the proposed method.

3.2 Improving Response Predictions with Different Matrix Rearrangements:

Transfer Path Analysis is an experiment-based procedure, and for this reason it is highly dependent on the quality of measurements taken. This topic has been discussed in detail in subchapter 2.5.1.1 where it has been shown that FRF measurements are prone to human errors and even when human error is minimized, the physical conditions of the system itself do not always allow performing the so-called perfect experiment. In the same subchapter the Coherence term has been explained and detailed.

In this section, the accelerance matrix will be rearranged to investigate the effect of the coherence values and also the cross coupling terms on the accuracy of the response prediction process. Calculation of the acceleration response at the steering wheel of the truck along the z direction is selected as the case study to demonstrate the effect of the proposed methods. Previously, Biermayer proposed “The Mountwise TPA” method [20] which consists of excluding the cross-coupling terms from other mounts as a means to improve the force identification process. The same method is mentioned in other papers [29, 30] together with the alternative of excluding all of the cross-couplings. In this study, 6 different matrix arrangements are investigated with the purpose of understanding the effect of coherence and also the cross coupling terms in the response prediction process.

1) **Standard matrix arrangement** – the accelerance matrix contains all of the measured data in its original shape.
2) **Overall Best FRF matrix arrangement** - The accelerance matrix is composed only with the FRFs that have the highest average coherence – Assuming that the matrix should be symmetric and one of the FRF measurements should be chosen, the one with biggest average coherence in the frequency spectrum is selected.
3) **Subinterval Best FRF matrix arrangement -** The accelerance matrix is symmetric and it is composed only with the FRFs that have the highest average coherence at every 5% of the frequency domain. For this case, the average coherence was computed at every 10 Hz interval and from each of this 5% intervals and the measurement with the highest average coherence in that subinterval was selected.
4) **Subinterval Best FRF matrix arrangement with cross-coupling omission** - Same as 3), the only difference being the cross-couplings are removed for every 10 Hz subintervals if the average coherence in that subinterval is lower than 90%.

   Note: The diagonal elements are always present in the matrix - only the <u>cross-couplings</u> can be removed.
5) **Diagonal matrix arrangement** – all of the cross-couplings are neglected
6) **“Mountwise TPA” matrix arrangement** – the accelerance matrix contains only the cross-coupling terms corresponding to the same mount connection. The cross coupling terms relating the mount-to-mount interactions are eliminated. The last

two cases are kept to verify the two alternatives for performing force identification that were proposed in the literature [20, 30].

The operational internal forces acting on the transfer paths are identified for all of the 6 cases above. Then, the forces are multiplied with the vector of transfer functions relating the cabin mounts to the steering wheel-Z sensor in order to obtain 6 different response predictions at that location.

The force identification was performed using direct inversion of the square matrix by following the steps for those 6 matrix rearrangement procedures. Then, the Moore-Penrose pseudo-inverse with a singular value rejection threshold of 2% of the biggest singular value was applied for the 6 methods such that the RMS error can be recalculated without being influenced by the possible ill-conditioning of the matrices.

The frequency band of 0-200 Hz is divided into 10 equal sub-intervals (every 20 Hz). For each of the subintervals, the ratio between the predicted and measured root mean square (RMS) values is calculated according to equation 7:

$$\frac{RMS_{pred}}{RMS_{meas}} = \frac{\sqrt{\frac{1}{\omega_{max}-\omega_{min}}\int_{\omega_{min}}^{\omega_{max}}\left|R_{pred}(\omega)\right|^2 d\omega}}{\sqrt{\frac{1}{\omega_{max}-\omega_{min}}\int_{\omega_{min}}^{\omega_{max}}|R_{meas}(\omega)|^2 d\omega}} \tag{7}$$

The results are tabulated in Tables 1 and 2, in order to compare the six methods and also the effect of using pseudo-inverse over direct inversion. Tables 1 and 2 show the ratios between the predicted and measured responses of the steering wheel acceleration in z direction in the IDLE configuration for the 6 different matrix arrangements using the pseudo inverse and direct inversion methods, respectively. A ratio of 1 or close to 1 means that the predicted response is very close to the measured one in that frequency band.

	20-40 Hz	40-60 Hz	60-80 Hz	80-100 Hz	100-120 Hz	120-140 Hz	140-160 Hz	160-180 Hz	180-200 Hz
M1	1.74	1.04	2.10	0.64	2.81	1.44	1.33	2.33	0.58
M2	1.23	1.03	0.82	0.79	0.55	1.23	0.98	0.64	1.35
M3	0.99	2.46	1.23	0.69	2.14	1.40	1.07	1.30	1.15
M4	0.54	2.46	1.23	0.69	0.47	1.40	1.08	0.77	1.53
M5	1.25	2.02	2.76	2.18	5.00	4.55	2.14	1.57	3.73
M6	1.37	2.04	2.41	2.30	5.00	3.61	5.00	3.45	4.29

Table 1: Ratio between the predicted and measured RMS values when predicting the response at Steering Wheel-Z for the IDLE condition with the pseudo-inverse

	20-40 Hz	40-60 Hz	60-80 Hz	80-100 Hz	100-120 Hz	120-140 Hz	140-160 Hz	160-180 Hz	180-200 Hz
M1	2.63	1.04	2.10	0.64	2.81	1.44	1.33	3.56	0.58
M2	2.75	1.06	0.82	0.79	0.55	1.23	1.39	0.63	1.63
M3	1.35	3.73	1.23	0.69	2.14	1.40	1.07	1.71	1.16
M4	0.74	3.73	1.23	0.69	0.47	1.40	1.08	1.03	1.77
M5	1.25	2.02	2.76	2.18	5.00	4.55	2.14	1.57	3.73
M6	1.37	2.04	2.52	2.30	4.99	3.61	5.00	3.45	4.29

Table 2: Ratio between the predicted and measured RMS values when predicting the response at Steering Wheel-Z for the IDLE condition with the direct inversion

The highlighted regions in Tables 1 and 2 show which method had the best prediction in the specified interval (the ratio closest to 1). For the case of Table 1, Method 2 has the best predictions in the interval of 40-160 Hz.

When pseudo inversion and direct inversion methods are compared, methods 2, 3 and 4 returns better results when compared to methods 1, 5 and 6 in all of the frequency bands.

The same methodology was repeated for the running truck on a straight track in the 10th gear to verify the outcomes of the current study. A similar trend was observed and methods 2, 3 and 4 returned better results. .When Tables 1 and 2 are investigated, in some of the frequency bands, there is an improvement (eg: especially for two of the subintervals 20-40 Hz and 160-180 Hz) when pseudo inversion method is used since it eliminates the ill-conditioning of the accelerance matrix. This can be also observed in Figure 36, the peaks around 40, 150 and 185 Hz were over predicted when the direct inversion method was used. The highest errors are obtained when methods 5 and 6 are used, and based on figure 37 it can be concluded that using the diagonal and mount-wise matrix arrangements have fairly limited application in the conditions where the far-field cross-couplings have close to no influence on the system. Method 2 results are slightly better than methods 3 and 4. This can be also observed in Figure 38 especially at frequencies around 55 Hz, 95 Hz, 125-130 Hz and 150-155Hz. Different measurements are used in methods 3 and 4 at different frequency bands and this can create discontinuities in the values of the transfer functions at the limits of the chosen frequency sub-intervals. For the case of method 4 removing cross-couplings based only on low-coherence criteria can also lead to neglecting important information. For that reason, method 2 will be used in the rest of the paper to demonstrate the effect of the selective cross coupling omission method.

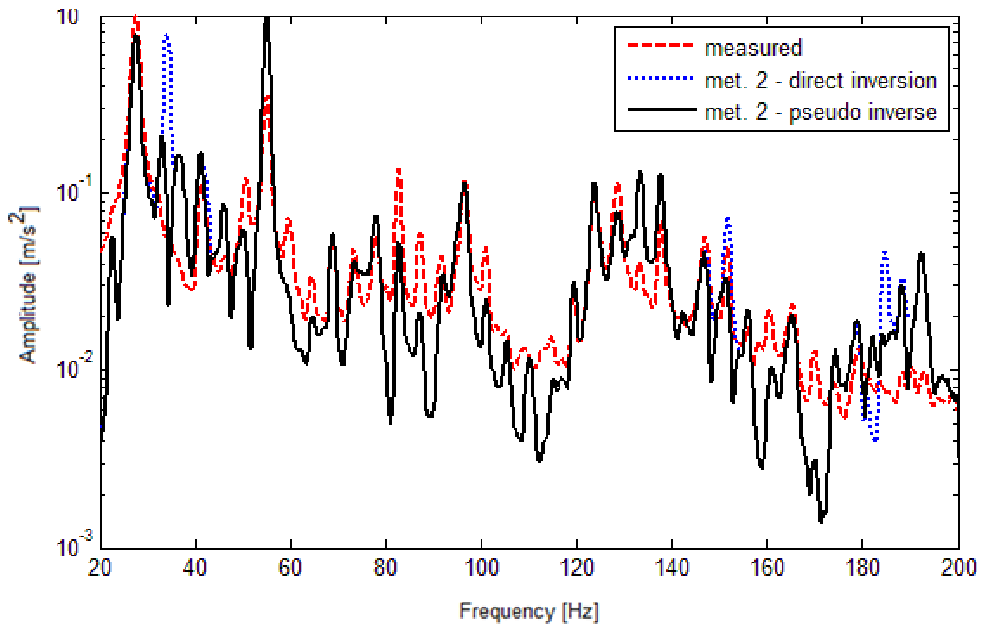

Figure 36: Comparison of Method 2 – direct inverse & pseudo-inverse prediction and measured response at Steering Wheel – Z in IDLE condition

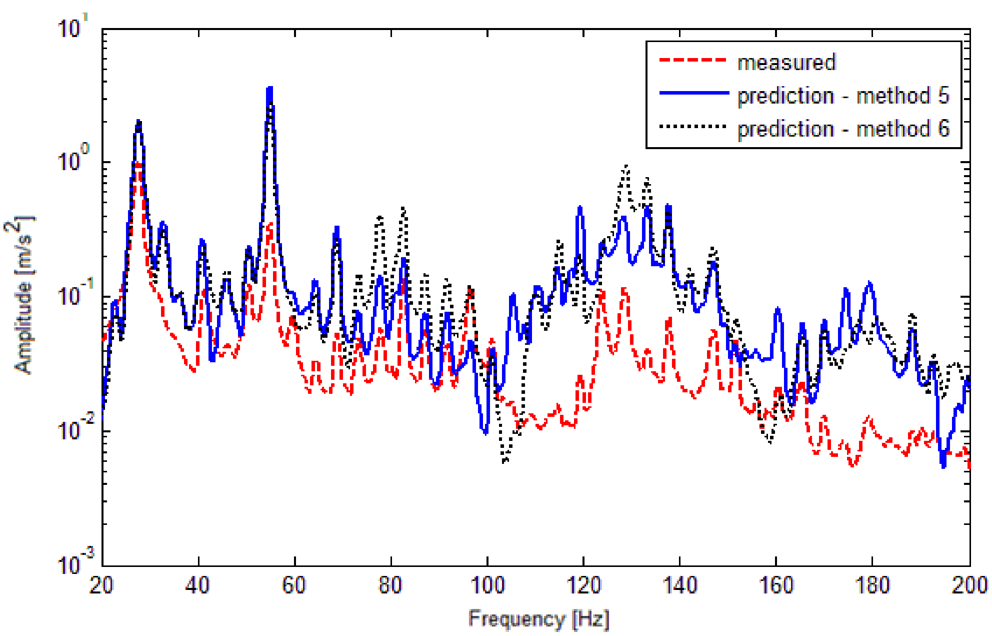

Figure 37: Comparison of Method 5 & 6 prediction and measured response at Steering Wheel – Z in IDLE condition

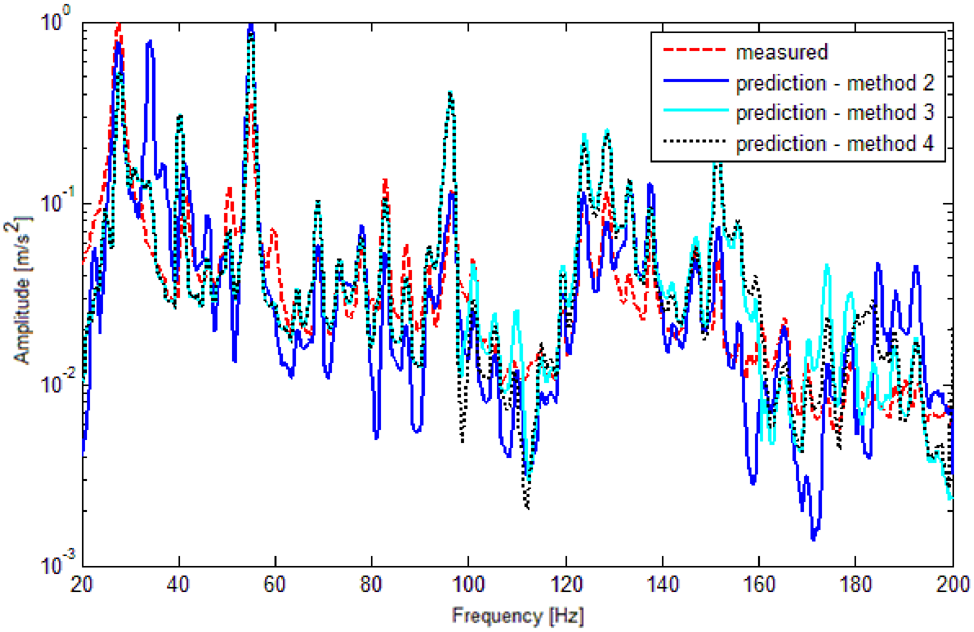

Figure 38: Comparison of Method 2,3 & 4 predictions and measured response

Omitting some of the cross-couplings in the accelerance matrix opens a whole new topic for discussion. In the above case studies, removing cross-couplings with coherence lower than 90% did not have a significant impact on the response prediction although it improved the end result in very small regions of the frequency band. The fact is that the coherence value is not the best term to characterize if the cross-couplings have a significant effect on the targeted operational response. It should be noted that FRF measurements with less than 90% coherence can still be considered good which means lower thresholds can be selected for omitting the cross coupling terms.

3.3 New approach to reducing condition numbers and over-estimation of forces

Further on, the cross-coupling omission in the accelerance matrix is studied with respect to another important aspect of the matrix inversion – the condition number. The theory related to the condition number has been presented in subchapter 2.6.1.1 where it has been concluded that if the measurement errors in matrix A are negligible and the matrix is well conditioned the internal force estimation becomes reliable. High condition numbers of the accelerance matrix often lead to the magnification of small response errors into large force errors.

3.3.1 The Moore-Penrose pseudo-inverse

Over determining the system of equations is the main method of reducing the ill-conditioning of matrix A which becomes rectangular. The internal forces acting on the paths are then computed by a least square method. In certain cases the over-determination of the system is not enough [29]. In the current literature [32,33], regularization techniques such as Singular Value rejection or Tikhonov regularization are used to reduce the error amplification of the matrix inversion process. The problem with these methods is that the optimum regularization parameter depends on both the condition number and measurement errors, making the selection of this parameter a difficult process.

The Moore-Penrose pseudo-inverse is the most common method used for the inversion of the accelerance matrix. The singular value decomposition of matrix A is:

$$A = U \cdot S \cdot V^H \tag{9}$$

where H represents the Hermitian transpose.

U is an orthogonal matrix composed out of to the eigenvectors of $A{\cdot}A^T$ and V is an orthogonal matrix composed out of to the eigenvectors of $A^T{\cdot}A$. The eigenvectors of $A^T{\cdot}A$ are calculated as such:

$$(A^T \cdot A - \lambda_r \cdot I) \cdot V_r = 0 \tag{10}$$

where V_r is the eigenvector of $I^T I$ for eigenvalue λ_r

The result for V is:

$$V = [v_1, v_2 \,..\, v_n] \tag{11}$$

where $v_1, v_2 \,..\, v_n$ form an orthonormal basis.

For U and V the first *m* eigenvalues $\lambda_1, \lambda_2 \,..\, \lambda_m$ are identical and non-zero.

$$u_p = \frac{1}{\sqrt{\lambda_p}} \cdot A \cdot V_p \tag{12}$$

where u_p is the eigenvector for eigenvalue λ_p and p=1,2,…,m.

By applying the Gram-Schmidt process to these vectors, U is obtained:

$$U = [u_1, u_2 \mathinner{..} u_n] \tag{13}$$

S is a diagonal matrix containing the singular values of matrix A and takes the form:

$$S = \begin{bmatrix} \sigma_1 & \cdots & 0 \\ \cdots & \ddots & \cdots \\ 0 & \cdots & \sigma_n \end{bmatrix} \tag{14}$$

where $\sigma_i = \sqrt{\lambda_i}$ and $\sigma_1 > \sigma_2 > \cdots > \sigma_n > 0$

The inverse of matrix A then becomes:

$$A^{+} = V \cdot S^{-1} \cdot U^{H} \tag{15}$$

where "+" indicates the pseudo-inverse. Small singular values σ_i have a large effect over the inverse of the matrix A. Rejection of small singular values is equivalent to replacing the $1/\sigma_i$ terms with 0. Singular value rejection can be a powerful tool for reducing error magnification. Threshold criteria based on estimates of error in either FRFs or operational responses have been explored but as mentioned before, neither is universally applicable.

3.3.2 The cross-coupling omission method

The role of the regularization methods is to replace the current problem with another problem, similar to the initial one, whose solution is less sensitive to perturbations [34]. In any regularization scheme, there is a regularization parameter which is a quantity that can be adjusted in order to change the degree of regularization of the solution. For values of this parameter at one end of its range, the solution is usually smoother, more similar to the default solution and less affected by noise on the data whereas for values of this parameter at the other end, the solution can be very sensitive to noise [35,36]. The proposed cross-coupling omission method intends to do the same thing for the case of inverting ill-conditioned matrices: by selective omission of the cross-couplings, the initial matrix slightly changes becoming better conditioned and allowing more accurate results for the inversion process.

Biermayer states that unconsidered cross-coupling terms can lead to a false identification of operational response at the target point with an error of up to 10 dB if the cross-coupling terms are not adequately included [30]. He then proposes the “Mountwise TPA" as a means of reducing the force over-estimations, but it was shown earlier that the method is not reliable when dealing with complex structures. As stated in the same paper, the increase in condition number is based on the low contributions of sources from other paths which usually cause low eigenvalues (noise) in the accelerance matrix. Many other researches in the field of matrices and matrix inversion [37-39] have covered the aspect of numerical optimization of eigenvalues or that of condition number of matrices, but from an engineering point of view, the force identification accuracy problem can be directly tied to the presence or absence of cross-couplings that make the matrix sensible to the inversion process.

With respect to this notion, sequential identification and omission of the low contributing paths is proposed.

For an accelerance matrix A of size *n x n*, the method can be described with the following steps:

1) Compute the condition number of matrix A
2) Temporarily replace $A_{ij}= 0$ and $A_{ji} = 0$; where $i \neq j$ and i,j = 1,2,.., n – incremented one by one.
3) Check if the condition number of the modified matrix is smaller compared to the condition number of matrix A at step 1.
4) If yes, permanently replace matrix A with the one where $A_{ij} =0$ and $A_{ji} =0$.
5) (i,j) reset to initial values (1,2)
6) Repeat steps 2) to 5) until a desired condition number of the matrix is reached or further decrease in condition number is impossible.

An alternative for the above method which may reduce the number of cross-couplings removed but requires more computational time can be established if step 3) is modified as follows:

1) Compute the condition number of matrix A
2) Replace $A_{ij} = 0$ and $A_{ji} = 0$; where $i \neq j$ and $i,j = 1,2,.., n$ – for the pair i,j where the reduction in condition number would be maximal;
3) For that specific pair of i,j - replace matrix A with the one where $A_{ij} = 0$ and $A_{ji} = 0$
4) Repeat steps 2) and 3) until a desired condition number of the matrix is reached or further decrease in condition number is impossible

Other variations of the standard method can also be considered. For example, if the condition number of the FRFs from the accelerance matrix is known, the removal of cross-coupling terms can be done in the order of the coherence values:

1) Compute the condition number of matrix A
2) Replace $A_{ij} = 0$ and $A_{ji} = 0$; where $i \neq j$ and $i,j= 1,2,.., n$ - for the pair i,j where the coherence value of the FRF defining the cross-coupling A_{ij} at that specific frequency is minimal
3) Check if the condition number of the modified matrix is smaller compared to the original condition number of matrix A. If yes, replace matrix A with the one where $A_{ij} = 0$ and $A_{ji} = 0$
4) Repeat steps 2) and 3) until a desired condition number of the matrix is reached or further decrease in condition number is impossible

3.3.2.1 Comparison of the three algorithms

The three algorithms presented are compared with respect to three criteria: the condition number reached, the number of pairs of cross-couplings removed and precision of response prediction for the case when the response at Steering Wheel-Z for the IDLE condition is predicted. As a running parameter for the algorithm, the targeted value for condition number is selected as 10. Following the results obtained in Chapter 3.2, matrix A is a 12x12 symmetric matrix where the FRF choice was based on the overall coherence value averaged in the frequency domain. The accelerance matrix shaped in this way has the condition number as shown in Figure 39:

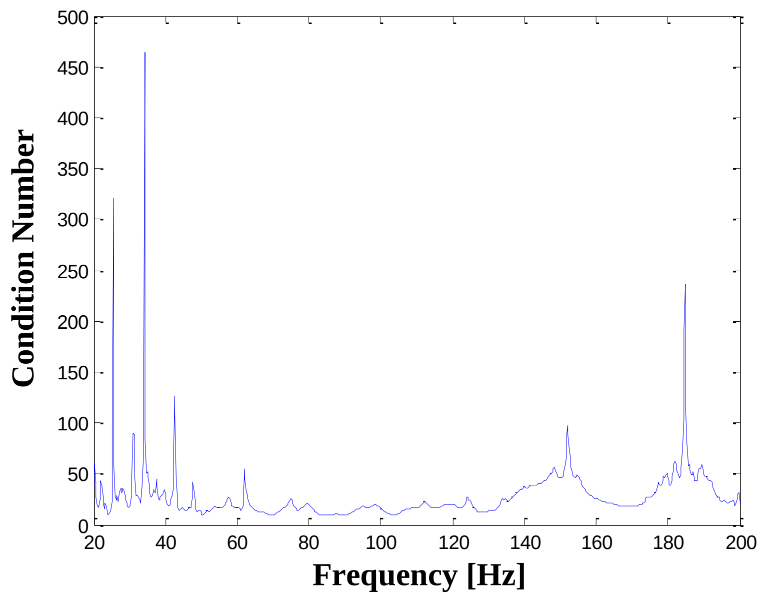

Figure 39: Original condition number of the accelerance matrix

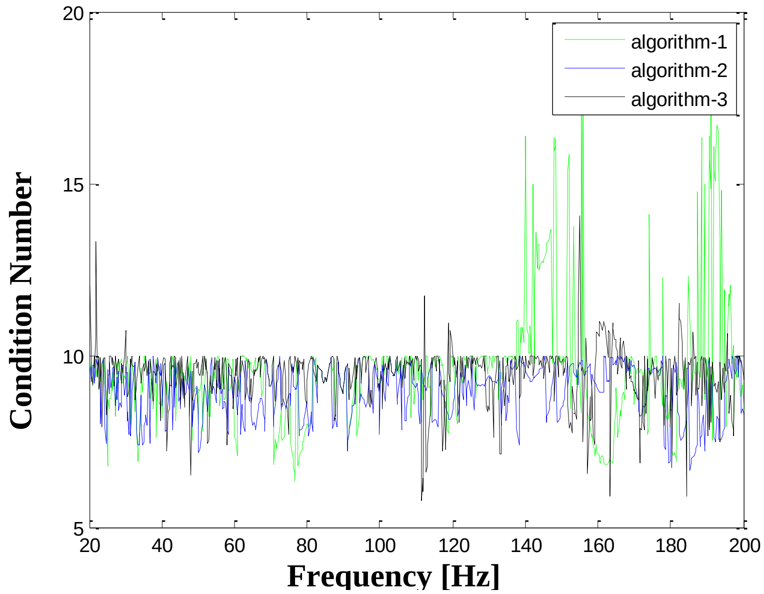

Figure 40: Condition number reached with the three algorithms

Between the three algorithms the first one is also the simplest. It sweeps the accelerance matrix in order, starting from the (1,2) – (2,1) cross-coupling pair until the (n-1,n) – (n,n-1) pair. It removes the first pair of cross-couplings that is found to reduce the condition number of the matrix and it starts sweeping again from the beginning until a targeted condition number is reached or no further beneficial removals are available. As shown in Figure 40, this algorithm did not manage to reach the condition number value of 10 in the entire frequency band, but the decrease was very significant and close to the desired target. With a really small exception, algorithms 2 and 3 have achieved the proposed goal.

There are a total number of 66 pairs of cross-coupling terms in a 12x12 accelerance matrix. Figure 41 shows the number of pairs that needed to be removed in order to reduce the condition number of the matrices to a value of 10. The higher the number of pairs removed to obtain a low condition number, the chance of removing significant cross-couplings increases. Setting a very low threshold for the condition number and removing too many of the cross-couplings can eventually lead to under-prediction of the targeted response. For this reason, the cross-coupling omission method should be used carefully and depending on the ill-conditioned state of the matrix different condition number thresholds should be attempted.

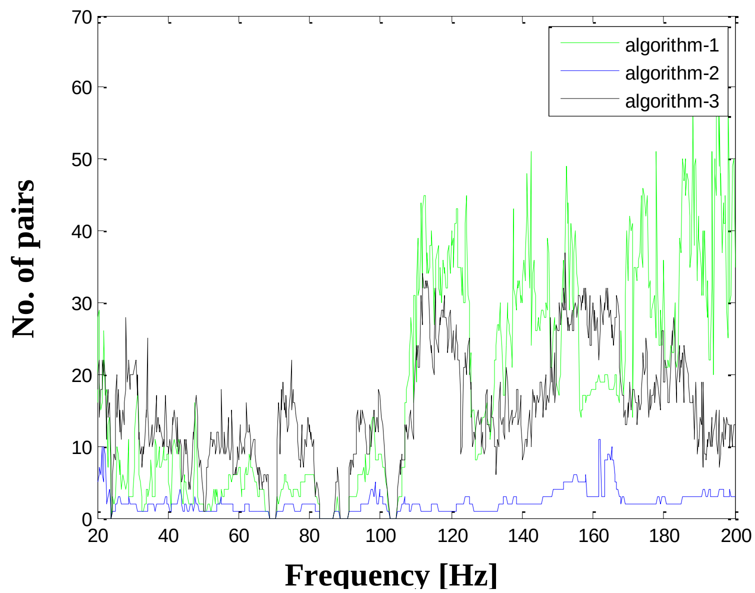

Figure 41: Pairs of cross-couplings removed from the accelerance matrix in order to obtain condition number value of 10

The second algorithm performs n·(n-1) sweeps of the accelerance matrix for each of the pairs of cross-couplings that is removed. As it can be seen in figure 41, using algorithm 2 results in a lot less cross-coupling pairs being removed but in exchange it requires more computational time. Removing less cross-couplings means that the ill-conditioning problem is solved while still using most of the information measured.

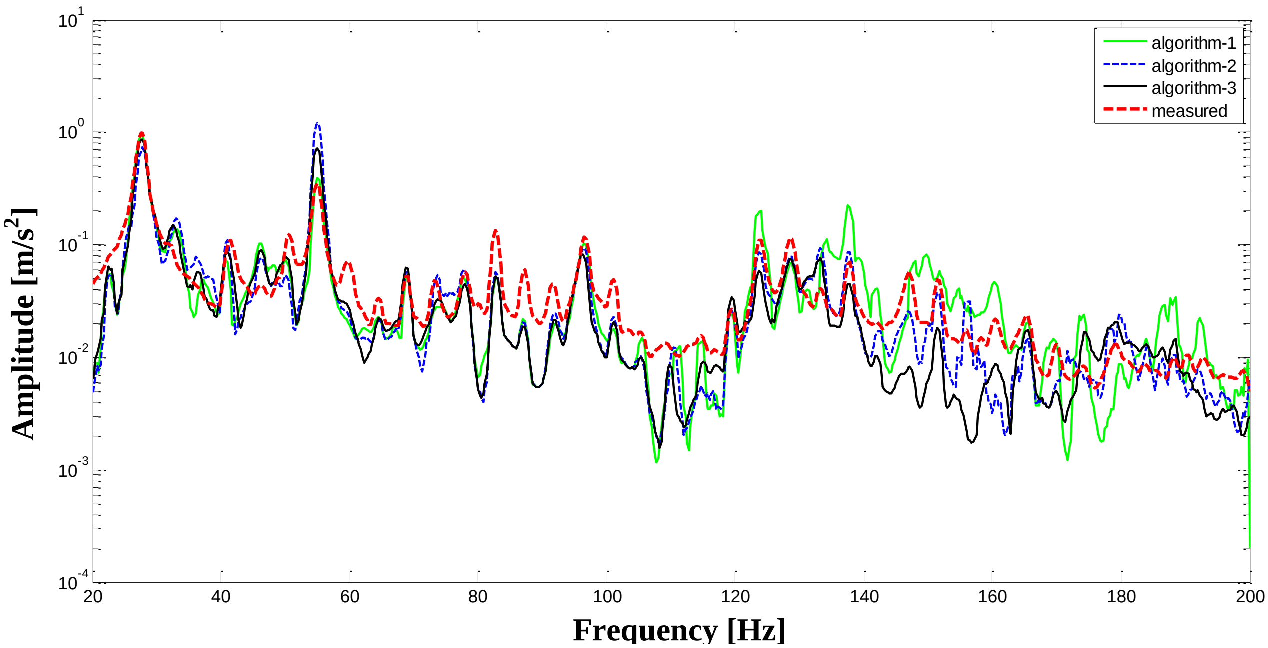

Figure 42: Comparison of predictions from the three algorithms

In terms of accuracy of predictions all of the algorithms are showing close results (figure 42). The first algorithm has a disorganized trend in the upper half of the frequency band either over predicting or under predicting the response. This phenomenon can be due to the number of pairs removed or because of the nature of the algorithm that starts removing cross-couplings always from the same path. With algorithm 3 the response is under predicted in the 140-160 Hz area while algorithm 2 gets closest to the measured acceleration in the whole frequency range. Because of the fact that it utilizes most of the data by removing only a few pairs of cross-couplings and due to its accurate response prediction, algorithm 2 proves to be the best out of the three. In the following chapter the response prediction obtained when using this algorithm will be compared to the prediction obtained with the More-Penrose pseudo-inverse.

3.3.3 Comparison of Moore-Penrose Pseudo-inverse and Cross-coupling Omission Method

In the current literature, there is no criteria for selecting threshold values for the condition number, where above and below that value, the system of equations can be considered well or ill-conditioned. Based on the initial values of the condition number presented in figure 39, a comparison of the response predictions obtained with the Moore-Penrose pseudo-inverse and the newly proposed method is presented for the cases when the condition number is reduced to 50, 30 and 10. For further information regarding the theory and application of the Moore-Penrose pseudo-inverse method, the reader is referred to Reference [28, 33]. For the Moore-Penrose pseudo inverse case, the singular value rejection thresholds are 2%, 3% and 10% of the highest singular value in order to obtain the maximum 50, 30 and 10 condition numbers over the entire frequency band. The comparison of the two methods is shown in figures 43, 44 and 45.

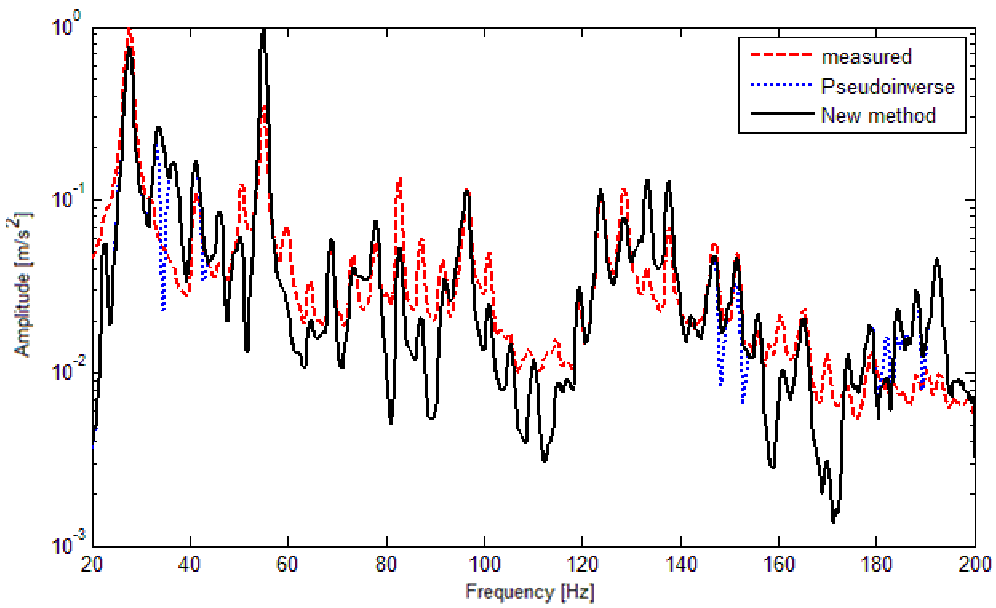

Figure 43: Comparison of response prediction at Steering Wheel Z in engine IDLE condition for the pseudo-inverse and new method when condition number is limited to 50

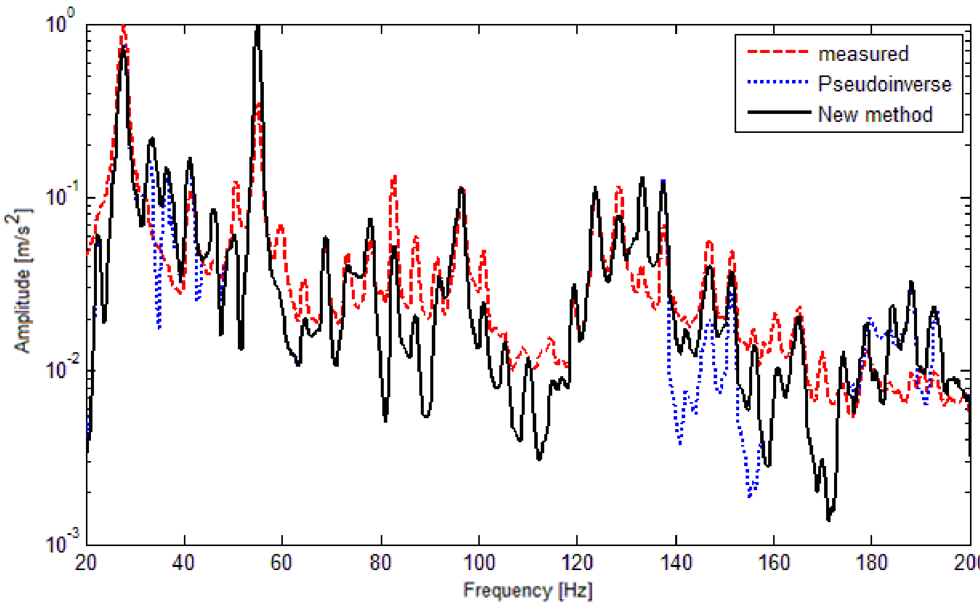

Figure 44: Comparison of response prediction at Steering Wheel Z in engine IDLE condition for the pseudo-inverse and new method when condition number is limited to 30

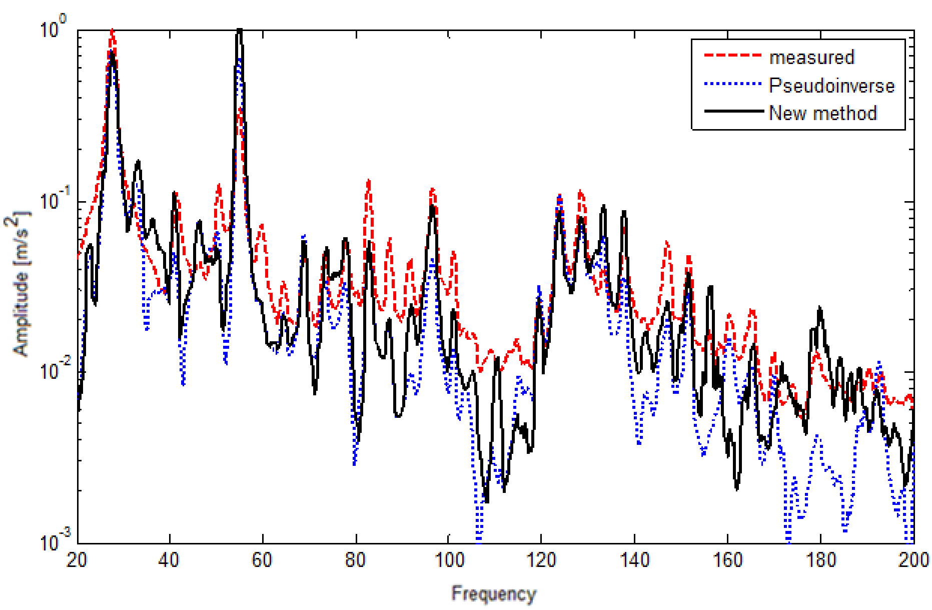

Figure 45: Comparison of response prediction at Steering Wheel Z in engine IDLE condition for the pseudo-inverse and new method when condition number is limited to 10

In figures 43 and 44, both the Moore-Penrose pseudo-inverse method and the newly proposed method did not improve the results significantly. The areas of the frequency band where the condition number of the accelerance matrix was already low remain unchanged. In figure 44, the prediction obtained with the newly proposed method matches better with the measured response in the 140-160 Hz region while in the other regions the predictions obtained look more or less the same when compared to the Moore-Penrose pseudo-inverse method. A much bigger difference can be seen when the condition number is lowered down to the value of 10. From Figure 45, it can easily be observed that the new method is resulting in much better predictions (especially between 60-180 Hz) than the case where the Moore-Penrose pseudo-inverse was used. The same metric in section 3.2 is used to compare the predictions of both methods and listed in Table 2. The same observations can be made when the metric values are investigated for the frequency bands provided in the table (Note that the first column gives the information regarding the condition number limit and method used). Equation 7 was used to generate Table 2 based on the predictions obtained with the pseudo-inverse and newly-proposed method for the 50, 30 and 10 condition number limits. As it could be observed from figure 12, the cross-coupling omission method returns better predictions when the condition number limit is lowered. This aspect is shown through the highlights in Table 2.

	20-40 Hz	40-60 Hz	60-80 Hz	80-100 Hz	100-120 Hz	120-140 Hz	140-160 Hz	160-180 Hz	180-200 Hz
CN50-Pinv	0.80	2.32	0.97	0.72	0.67	1.27	0.81	0.86	2.34
CN50-New	0.83	2.32	0.97	0.72	0.67	1.27	0.91	0.85	2.38
CN30-Pinv	0.77	2.32	0.97	0.72	0.67	1.26	0.42	0.83	1.91
CN30-New	0.78	2.32	0.97	0.72	0.67	1.25	0.73	0.83	1.97
CN10-Pinv	0.75	1.66	0.74	0.40	0.52	0.84	0.44	0.55	0.54
CN10-New	0.74	2.94	0.93	0.60	0.58	0.96	0.77	0.77	1.17

Table 3: Ratios between the predicted and measured RMS values when predicting the response at Steering Wheel-Z for the IDLE condition with the pseudo-inverse and new method

The advantage of the proposed cross-coupling omission method for improving the force identification and response prediction is the accelerance matrices do not have to follow a strict rule related to the cross-couplings that should be included. Previous methods that suggest using a Diagonal Matrix or matrices containing the cross couplings coming from the same mount are limited in this aspect. Furthermore, the cross-coupling omission method is based on selecting the target condition number of the accelerance matrix which is a more solid and far less complex procedure compared to the singular value rejection threshold. Another advantage is that the algorithm for omitting the cross-couplings can be easily adapted to the user's needs depending on the cross-couplings that should be neglected or not. The proper selection of the cross-couplings omitted is done through several iterations of the algorithm. If the accelerance matrix contains many elements, then computational time also increases, making it a more computationally demanding process than the singular value decomposition.

CHAPTER 4

DISCUSSION & CONCLUSION

Transfer path analysis (TPA) is a well-developed procedure that allows tracing the flow of vibration and/or sound energy from a source, through multiple transfer pathways, to a given receiver location. In this thesis, a design methodology that employs experimental TPA methods to predict the vibro-acoustic performance of a truck cabin is presented. The analysis tools and the methodology presented provide a systematic and quantitative way to investigate the end-to-end vibro-acoustic performance of such systems, perform TPA, and identify the critical components of the system that degrade the performance. The TPA method is employed in order to predict the sound pressure level inside a prototype heavy duty truck cabin and the vibration level on the steering wheel.

The TPA analysis was performed considering the effects of the cabin suspension and engine mounts where the engine was running in IDLE condition and also for a high gear run-up on the track. First the operational internal forces are calculated using the matrix inversion method, then the internal forces are multiplied with the corresponding FRF’s to calculate the required vibration or noise responses at the predefined locations. For the validity of the predicted results, coherence of the collected data and the condition numbers of FRF matrices are investigated so that the accuracy of the predicted results can be quantified for the frequency band of interest. The TPA also quantifies the contribution of each individual path such that problematic paths can be identified. The predictions of the total response are compared with the experimentally measured noise and vibration data such that the TPA predictions are validated. The vibration and noise predictions compared well with the measured ones for the idle condition for both the cabin and engine TPA. The acceleration predictions obtained for the high gear engine run up condition are good only for the cabin TPA case. During the wide open throttle run-up, many secondary paths have influence on the accelerations and sound pressures inside the cabin. The vibrations coming from the road through the vehicle's suspension along with the aerodynamic noise corrupts the results for the engine TPA. Sound pressure levels are over-predicted in some frequency ranges due to possibly unreliable NTF data. But although the input data is slightly corrupted, the trend of the estimated response level is similar to the measured one. Contribution of the mounts to the accelerations and sound pressure levels are shown for the ranges where response predictions are good and condition numbers are low.

TPA results show that the methods that were developed can be used to improve the vibration and noise level inside the passenger cabin of heavy duty trucks. Although some of the standard commercial tools and well established techniques are utilized in this study, the integration of the results of such analysis tools and experimental findings is unique and the methods that were proposed provide a lot of insight to the design engineers.

A MATLAB toolbox was developed to perform TPA and the details are included in the Appendix. The developed toolbox is versatile and easy to use for performing Transfer Path Analysis. It has an intuitive graphical interface, it allows the user to input data measured on any type of complex structure, it investigates the imported data and as a result of TPA, it provides information such as response prediction and path contribution for targeted locations.

The study presented in chapter 3 proposes a new approach to improve the current methods of indirect force identification through matrix inversion. Measurements are taken on a heavy duty Ford truck for performing TPA to obtain the operational forces at the cabin mounts and predict the in-operational responses on the steering wheel. Initially, six different accelerance matrix arrangements based on the coherence knowledge of the FRFs are tested in order to obtain the best predictions for the measured acceleration response. Two of the six cases are meant to prove that in a complex structure, neglecting all of the cross couplings or creating a specific rule for omitting cross-couplings such as the case of

“Mountwise TPA” does not improve the prediction of the responses. The results of the study have shown that the best response predictions are obtained when the accelerance matrix is strictly symmetric and the FRF selection was done based on the overall frequency averaged coherence. It is shown that cross-coupling omission of the low coherence measurements does influence the end result and should always be considered.

A new approach for enhancing the ill-conditioning state of the accelerance matrices is also introduced in chapter 3. It is shown that selective cross-coupling omission greatly improves the response predictions. An algorithm for selective-cross coupling omission is presented which targets the decrease of the condition number of the accelerance matrices. When compared with the singular value decomposition techniques with singular value rejection threshold for overcoming the ill-conditioning of the matrices, the newly proposed method resulted in better in-operational response predictions. The cross-coupling omission method has two main advantages over the common regularization techniques used in present: it uses the condition number as a running parameter and the cross-coupling omission algorithm can be easily adapted to various situations depending on the cross-couplings that should or should not be included in the force identification process.

For future studies, new and improved algorithms for selecting the omission of cross-couplings can be developed. The cross-coupling omission method for improving the force identification and response prediction can also contribute to future studies that follow to investigate at which values of the condition number the force identification becomes optimal.

BIBLIOGRAPHY

[1] Visser, R. (2009). Virtual Transfer Path Analysis at Daimler Trucks. SAE International.

[2] Krishna R. Dubbaka, F. J. Z. a. S. U. H. (2003). Application of Noise Path Target Setting Using the Technique of Transfer Path Analysis. Noise & Vibration Conference and Exhibition. Traverse City, Michigan.

[3] Genuit, K. and J. Poggenburg (1999). The Design of vehicle Interior Noise Using Binaural Transfer Path Analysis.

[4] Sturesson, P.-O., et al. (2012). "N&V Integration and Optimization of Driveline Using Transfer Path Analysis." SAE International.

[5] Koizumi, T., et al. (2009). "A Measures Planning Method by Analysis of Contribution of the Vibration Transfer Path." SAE International.

[6] Knapen, P. L. (1999). Transfer Path Analysis related to booming, performed on a car.

[7] Plunt, J. (1998). Strategy for transfer path analysis (TPA) applied to vibro-acoustic systems at medium and high frequencies. International Conference on Noise and Vibration Engineering. Leuven, Belgium.

[8] Vecchio, A., et al. (2005). Experimental Transfer Path Analysis of a hybrid bus. SAE 2005 Noise and Vibration. Traverse City, Michigan.

[9] Vinod k. Singh, N. W., Vincent D. Monkaba, Jason R. Bloughand Geoffrey Gwaltney (2001). Powertrain Transfer Path Analysis of a Truck. International Truck and Bus Meeting and Exhibition. Chicago, Illinois.

[10] Bograd, S. (2005). Application of TPA to Hydraulic Systems. Mechanical Engineering, UNIVERSITY OF CINCINNATI. Masters of Science.

[11] Janssens, K., et al. (2009). A Novel Transfer Path Analysis Method Delivering a Fast and Accurate Noise Contribution Assessment. Symposium on International Automotive Technology. India.

[12] Janssens, M. H. A. and J. W. Verheij (2000). "A pseudo-forces methodology to be used in characterization of structure-borne sound sources." Applied Acoustics 61.

[13] Haste, F. and A. Nachimuthu (1998). Calculating Partial Contribution Using Component Sensitivity Values - A Different Approach to Transfer Path Analysis. Noise and Vibration Conference & Exposition. Traverse City, Michigan.

[14] Sitter, G. D., et al. (2004). Experimental Transfer Path Analysis Without Disassembling the Structure. Conference & Exposition on Structural Dynamics. Dearborn, Michigan.

[15] Transfer Path Analysis - The qualification and quantification of vibro-acoustic transfer paths, LMS International

[16] Janssens K. GP, Van der Auweraer H. (2008) Operational path analysis: a critical review,. ISMA 2008, September 2008.

[17] de Klerk D, Ossipov A. (2010) Operational transfer path analysis: Theory, guidelines and tire noise application. Mechanical Systems and Signal Processing,24: 1950-1962.

[18] De Sitter G, Devriendt C, Guillaume P, Pruyt E. (2010) Operational transfer path analysis. Mechanical Systems and Signal Processing,24: 416-431.

[19] Janssens K, Gajdatsy P, Gielen L, et al. (2011) OPAX: A new transfer path analysis method based on parametric load models. Mechanical Systems and Signal Processing,25: 1321-1338

[20] Werner Biermayer , Franz Brandl , Robert Hoeldrich, Alois Sontacchi , Stephan Brandl. (2008) - Efficient Transfer Path Analysis for Vehicle Sound Engineering. Journal Society of Automotive Engineers

[21] Thite AN, Thompson DJ. (2003) The quantification of structure-borne transmission paths by inverse methods. Part 1: Improved singular value rejection methods. Journal of Sound and Vibration

[22] Thite AN, Thompson DJ. (2006) Selection of response measurement locations to improve inverse force determination. Applied Acoustics,67: 797-818.

[23] Verheij J. (1982) Multipath Sound Transfer from Resiliently Mounted Shipboard Machinery. Institute of Applied Physics. pp. 294. TNO-TH, Delft, Netherlands.

[24] J. Plunt. (2005). Finding and fixing vehicle NVH problems with transfer path analysis. Journal of Sound and Vibration.

[25] Starkey J. MG. (1989) On the ill-conditioned nature of indirect force measurement techniques. International Journal of Analytical and Experimental Modal Analysis

[26] Van der Linden P. FH. (2004) Comparing inverse force identification and the mount stiffness force identification methods for noise contribution analysis. ISMA Conference September 2004

[27] Verheij JW. (1997) Inverse and reciprocity methods for machinery noise source characterization and sound path quantification, Part 1: sources. International Journal of Acoustics and Vibration 2, 11-20

[28] Verheij JW. (1997) Inverse and reciprocity methods for machinery noise source characterization and sound path quantification, Part 2: transmission paths. International Journal of Acoustics and Vibration 2, 103-112

[29] M.H.A. Janssens, J.W. Verheij, D.J. Thompson, (1999) The use of an equivalent forces method for the experimental quantification of structural sound transmission, Journal of Sound and Vibration 226, 305–328.

[30] W. Biermayer FB, R. Höldrich, A. Sontacci, S. Brandl, W. Fliesser. (2007) Sound Engineering based on Source Contributions and Transfer Path Results. Journal of Society of Automative Engineers of Japan.

[31] Mirko Reising, Ferit Küçükay (2013) - Hybrid acoustic synthesis – Assessment of rear final drives in an early stage of development, on the basis of transfer path analyses and test bench measurements, Applied Acoustics

[32] Thite AN. (2003). Inverse Determination of Structure-borne Sound Sources. PHD Thesis, University of Southampton

[33] Thite AN, Thompson DJ.(2003). The quantification of structure-borne transmission paths by inverse methods. Part 2: Use of regularization techniques. Journal of Sound and Vibration

[34] Silvia Nosches , Lothar Reichel (2012). Inverse problems for regularization matrices. Numerical Algorithms

[35] M. Bertero. (1986). Regularization methods for linear inverse problems

[36] Andrew E. Yagle. Regularized Matrix Computations

[37] E. Mengi, E.A Yildirm, M. Kilic (2014) - Numerical optimization of eigenvalues of hermitian matrix functions. Society for Industrial and Applied Mathematic

[38] Tullio Zolezzi (2011) - Condition number theorems in linear - quadratic optimization. Numerical Functional Analysis and Optimization

[39] Zhaosong Lu (2010) - Minimizing Condition Number via Convex Programming. Society for Industrial and Applied Mathematics

APPENDIX

TRANSFER PATH ANALYSIS MATLAB TOOLBOX

A.1 Introduction

The developed toolbox is a versatile and easy to use tool for performing Transfer Path Analysis. The software was developed in MATLAB environment and it has an intuitive graphical interface. It allows the user to input data measured on different complex structures, investigates the imported data and as a result of a TPA analysis, it provides information such as response prediction and path contribution for targeted locations.

A.2 Requirements

To be able to run the TPA Toolbox, the correct version of Matlab Compiler Runtime must be installed in advance. The installer for Matlab Compiler Runtime should be the same version as the one used in programming the Software (version 2011a).

A.3 Software main interface

In figure A1 the main software interface is presented together with the important sections in the interface. Later on, each individual section will be described together with the button functionalities.

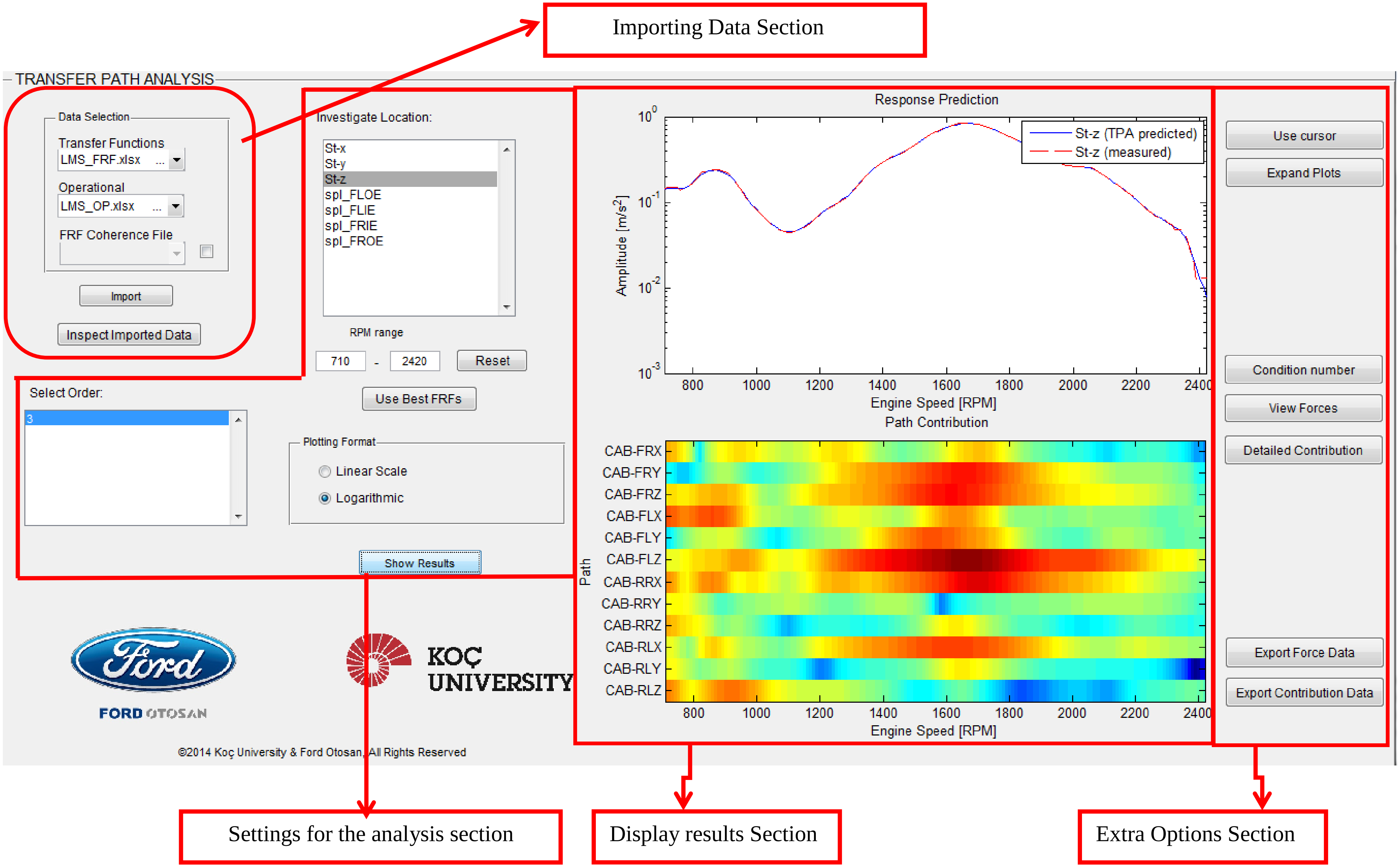

Figure A 1: TPA Software Main Interface

A.4 Importing Data

Before running an analysis the measured data needs to be organized in a specific way. The Frequency Response Functions are organized in one Excel file and the Operational Data are organized in a separate Excel file. An Excel file containing the coherence data is optional. This process of creating the Excel files is described in one of the chapters below. The excel files need to be placed in the same folder with the executable file of the TPA Software.

When the program is opened the interface looks similar to figure A2:

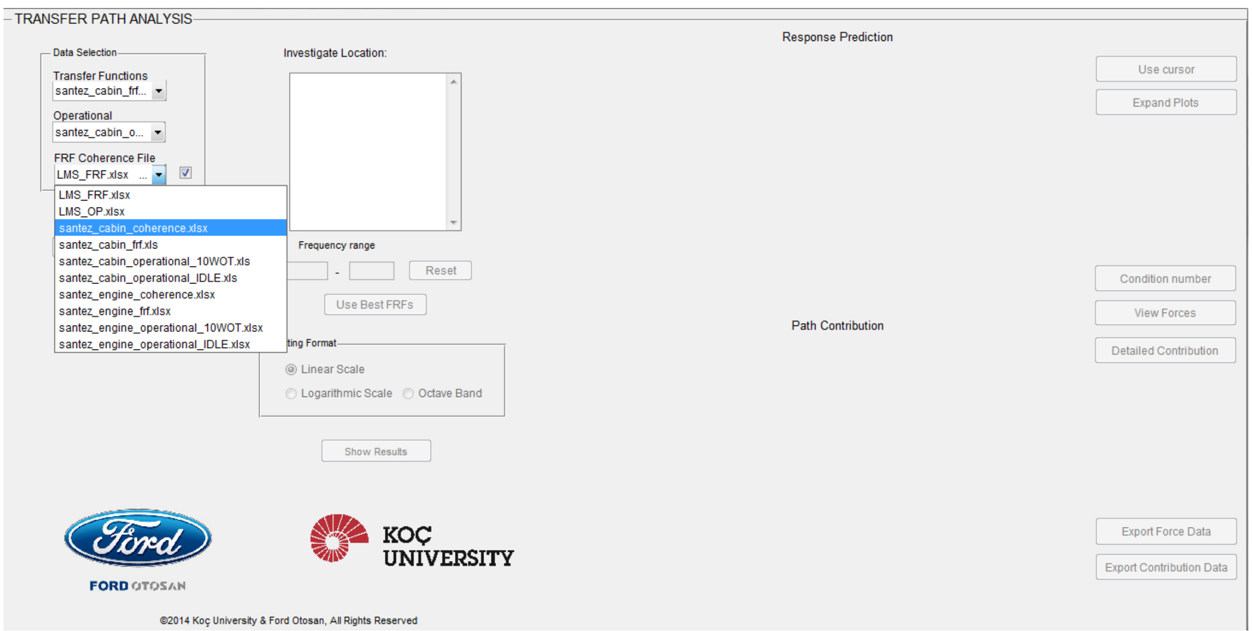

Figure A 2: Interface at Startup

The Excel files containing the desired Transfer Functions and the one containing the desired Operational Responses should be selected at this step. Importing the FRF Coherence File is optional. In order to be able to import it, the checkbox right to the popup menu should be ticked. After the file selection is done, the “Import” button should be pressed.

A.5 Inspecting the imported data

After importing a set of data, the "Inspect Imported Data" button becomes available. If the user desires to check some of the FRFs or Operational Acceleration/SPL he can do that by pressing the "Inspect Imported Data" button. There is also an option of comparing an FRF with the one measured from the opposite direction. Once the "Inspect Imported Data" button is pressed, a new menu will pop-up (Figure A3).

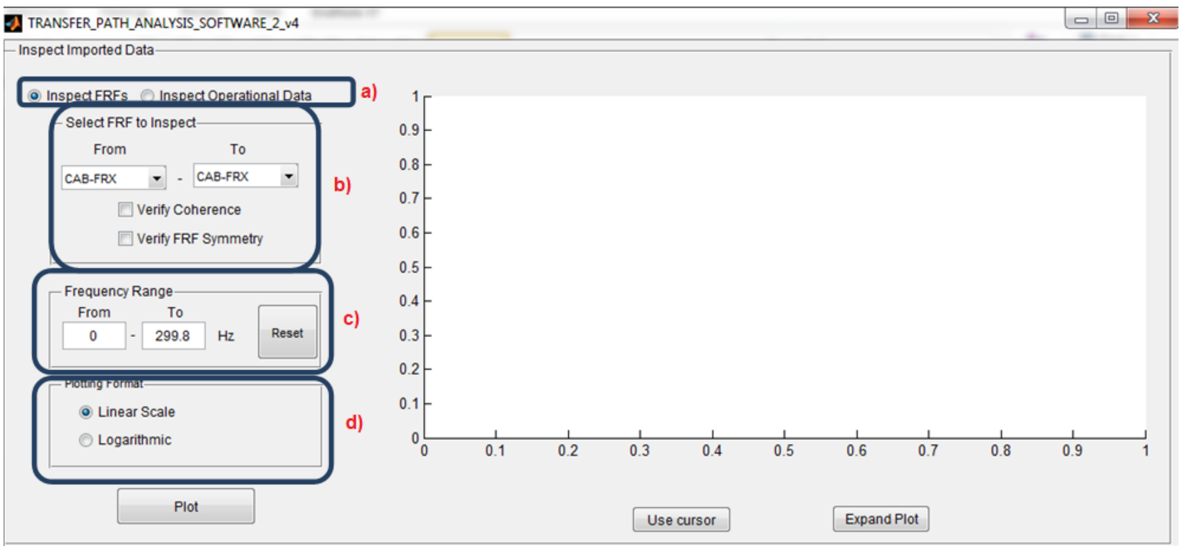

Figure A 3: Data inspection interface

At first, there are 2 options: either "Inspect FRFs" or "Inspect Operational Data". Depending on the choice the b) menu will change.

if "Inspect FRFs" was selected at point a) the interface looks like figure A4:

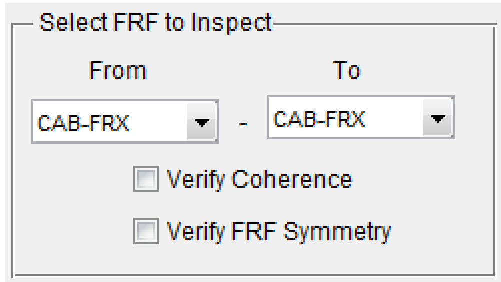

Figure A 4: b) menu when "Inspect FRFs" was selected at point a)

The menu allows the selection of the FRF to be inspected by choosing the “From” and “To” locations. If “Verify Coherence” tick box is checked – the coherence of the selected FRF will be plotted. The d) menu will also change as described below. If “Verify FRF Symmetry” tick box is checked then the selected FRF will be plotted together with the FRF measured from the opposite direction

If “Inspect Operational Data” was selected at point a), the b) menu looks like Figure A5:

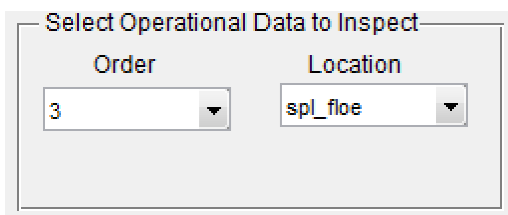

Figure A 5:b) menu when "Inspect Operation Data" was selected at point a)

If the imported data is order-cut data the Order selection will be available. The menu allows selecting the desired Order and Location for the Operational Data to be inspected.

Depending on the type of data the user wants to inspect the software has the option of selecting the range of visualization either in Hz or RPM (figure A6). By default, the start and end values for these ranges are the ones imported from the Excel file. The "Reset" button will bring the numbers in the boxes to the default values.

Figure A 6: c) menu depending on the type of data inspected

If the selected data for plotting is a FRF, NTF or acceleration the plotting options will be either "Linear" or "Logarithmic". If the selected data for plotting is a Sound Pressure Level the plotting options will be "Linear", "Decibels" or "Octave Band" (figure A7).

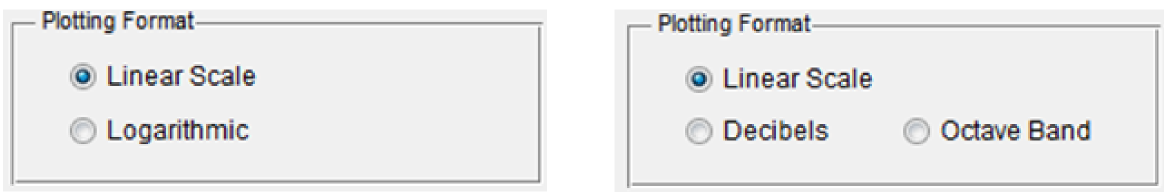

Figure A 7: d) menu depending on the type of data imported

If "Verify Coherence" tick box was selected at point b), then this menu will be replaced with the "View Coherence Metric" (figure A8). By pressing this button a matrix with the average coherences in the selected range will be plotted.

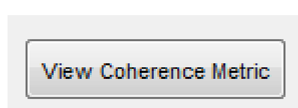

Figure A 8: View Coherence Metric Button

After all the selections from a)-d) are correctly selected and the “Plot” butto is pressed, the result will be displayed on the right side of the screen.

If “Use cursor” button is toggled, it will allow the user to check different values on the plot.

The “Expand Plot” Button will open a new window of the current plot. This will allow the user to resize the image or save the plot as a .JPG file.

A.5.1 Inspected data – plot examples

A series of plotting examples resulted from the data-inspection process are presented in figures A9 to A14. These contain simple FRF and symmetric FRF plots, simple coherence plots, coherence metric plots and operational data plots in simple/logarithmic scale and in the octave band.

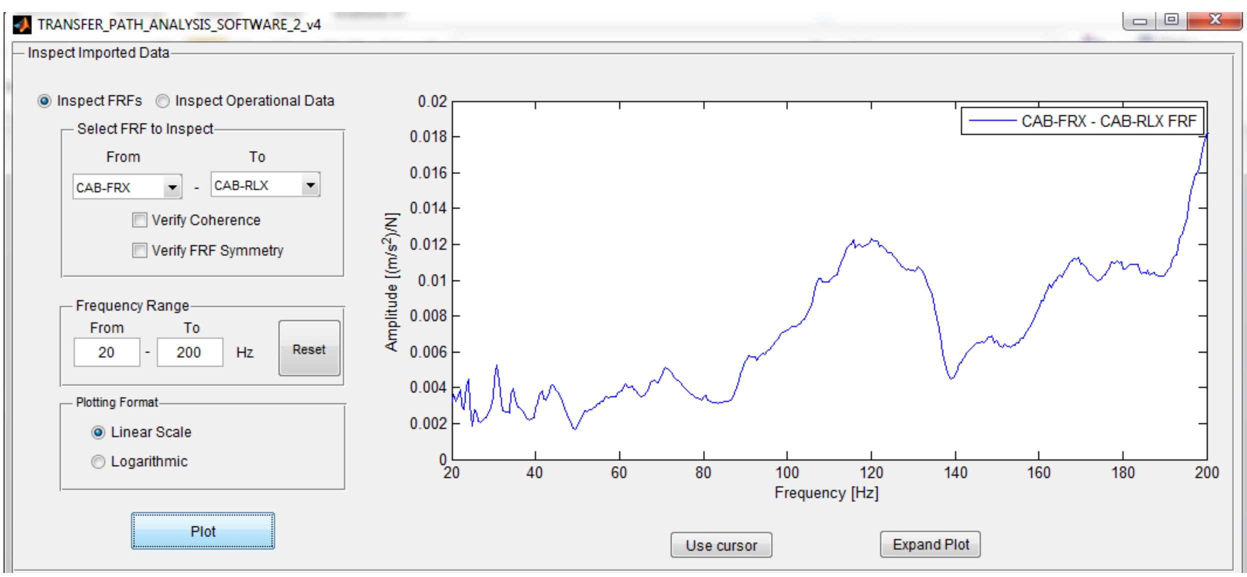

Figure A 9: Simple FRF plot

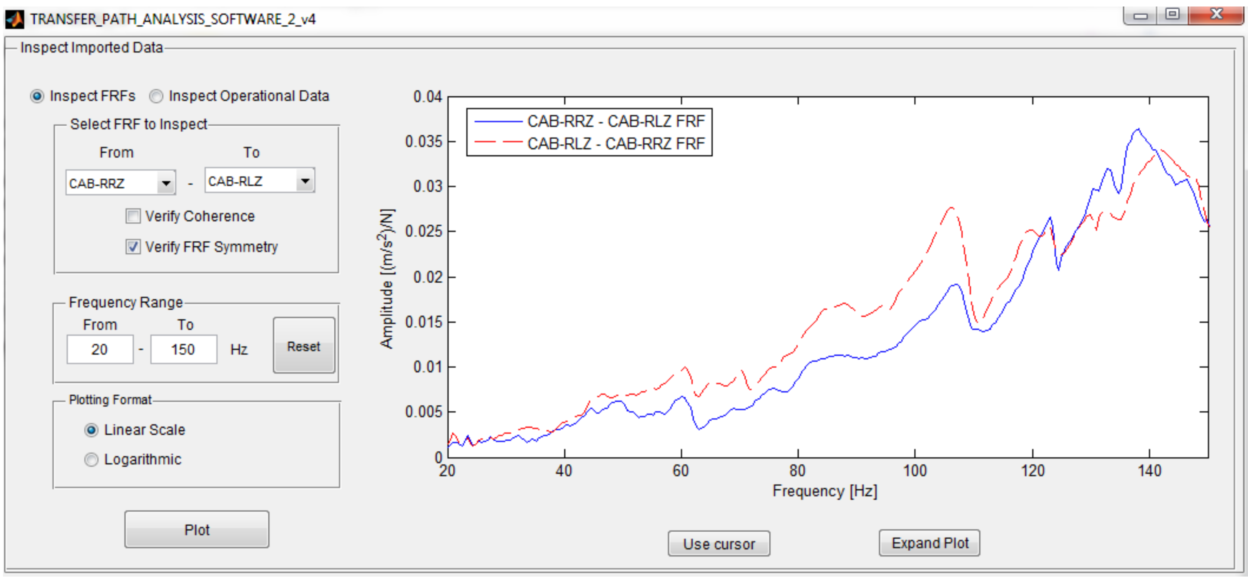

Figure A 10: A-to-B and B-to-A FRF symmetry verification

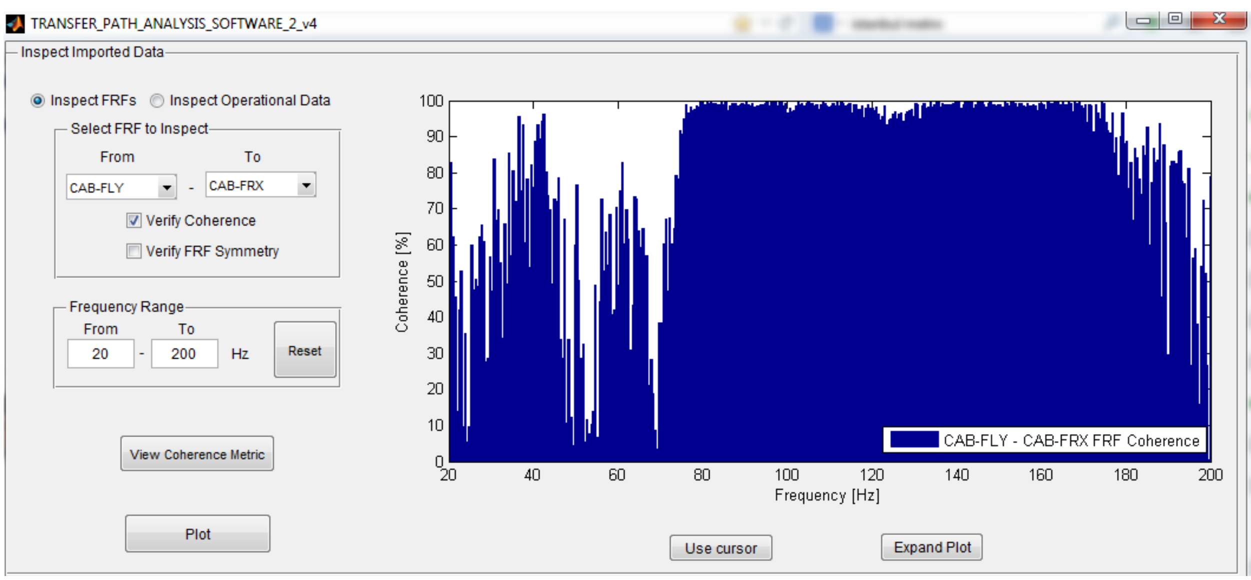

Figure A 11: FRF coherence Plot

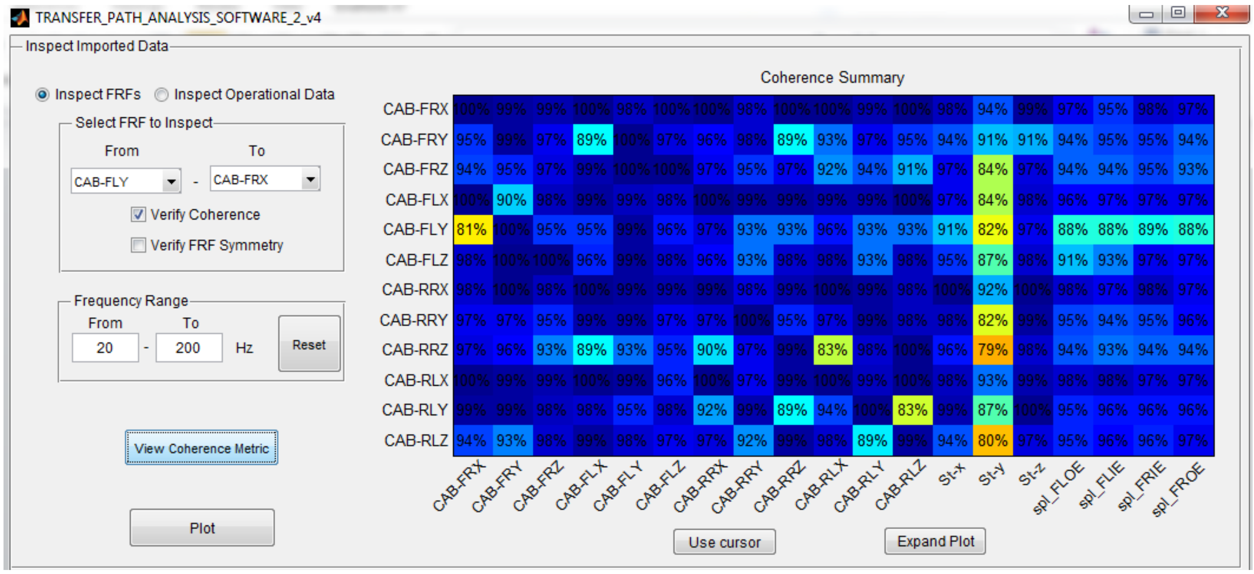

Figure A 12: Coherence Metric Plot

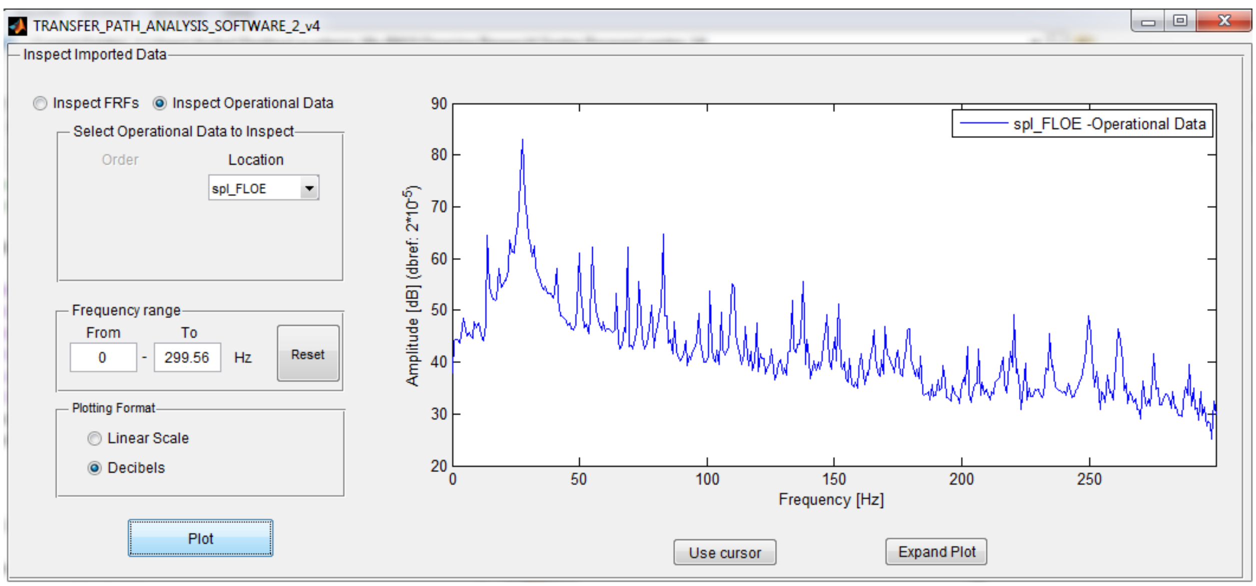

Figure A 13: Operational Data Plot

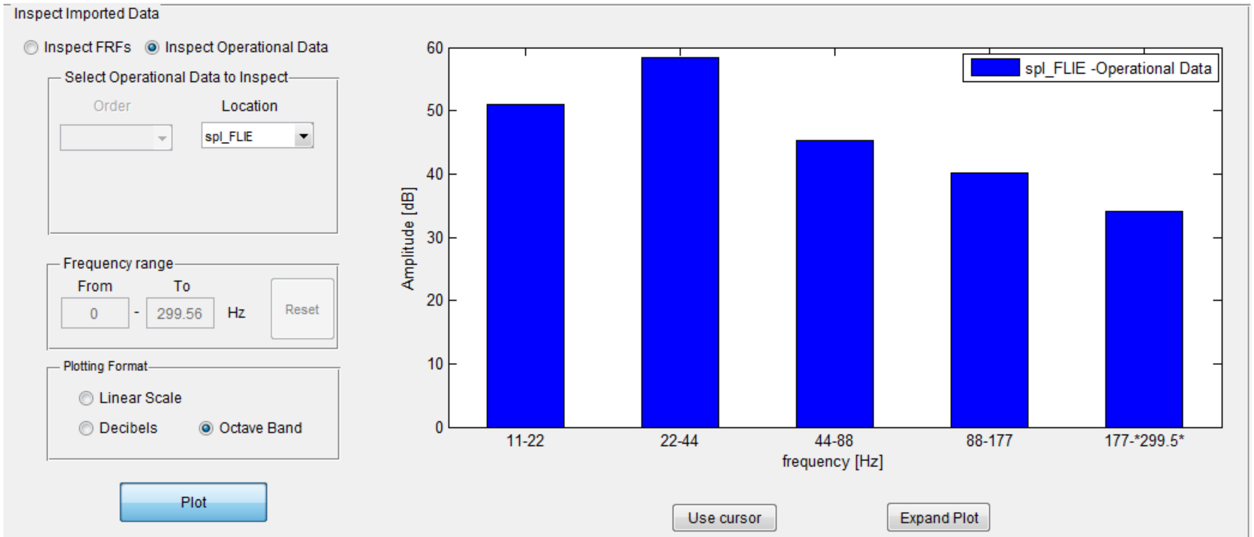

Figure A 14: Octave band plot for Sound Pressure Level

A.6 Running an Analysis

After the Transfer Functions and Operational Responses files have been imported, the settings for the analysis will unlock (as shown in Figure A15).

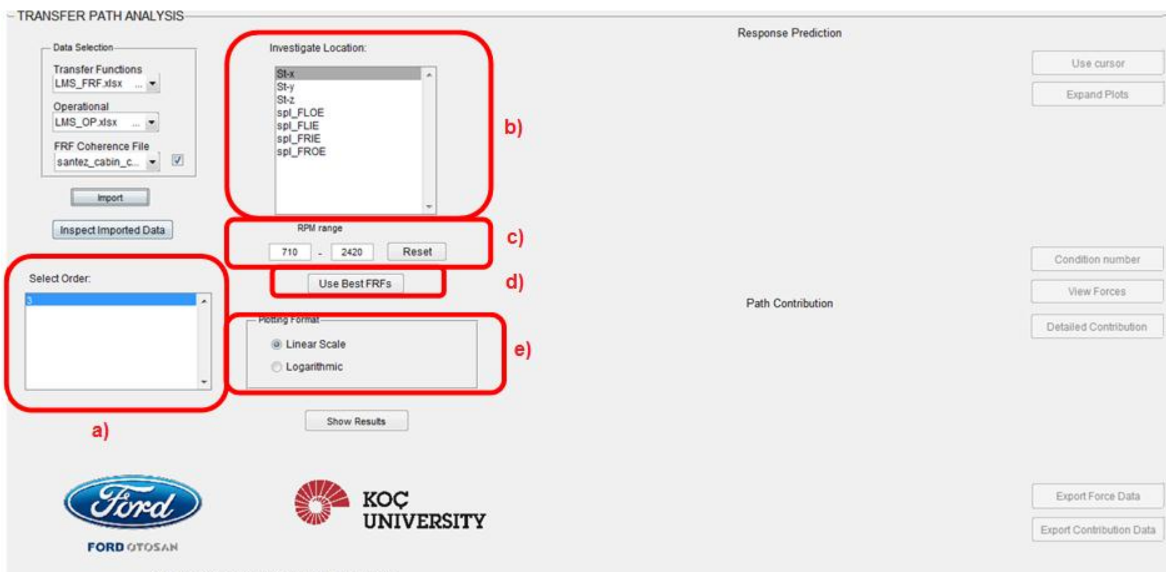

Figure A 15: Main interface after importing data

If order-cut data is imported, the a) submenu will be available and it will allow the user to select the order of the data that will be inspected.

The b) submenu shows the target locations for which response prediction and path contribution can be performed.

The c) submenu is used for selecting the range in RPM/Frequency for the inspected data. By default it will have the values imported from the input files.

d) is a toggle button that will make the matrices involved in the TPA analysis symmetric. It means that it will only use the A-to-B FRFs and not the B-to-A FRFs. IF the Coherence Excel File is imported, the toggle button name will be “Use Best FRFs”. When pressed, the analysis will automatically select the FRFs with the highest coherence averaged in the frequency band.

In the e) section, the plotting format can be selected. The options will either be Linear Scale and Logarithmic Scale for the acceleration predictions and Linear Scale and Decibels / Octave Band for the SPL prediction

After all the selections from a)-e) are done the “Show Results” button can be pressed. The results of the analysis are now displayed on the right side of the screen.

A.7 Other Options

After the “Show Results” button is pressed, the main interface will look as in Figure A16:

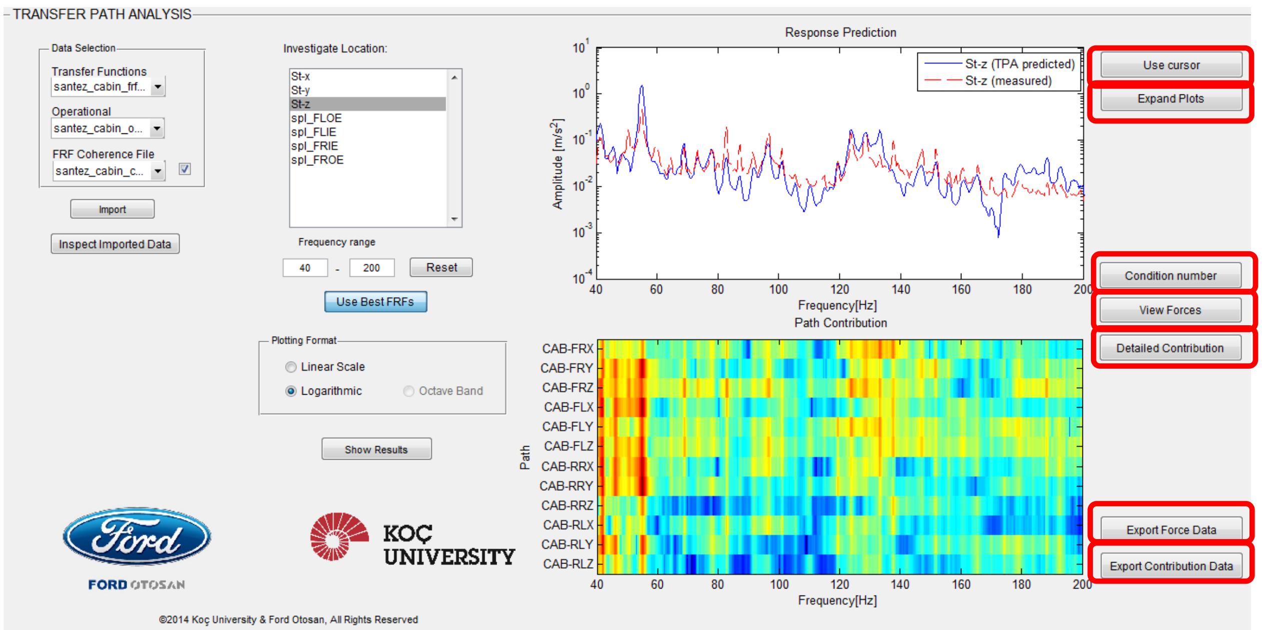

Figure A 16: Main interface after displaying the results

“Use cursor” toggle button allows the user to inspect the values on the plots.

“Expand Plots” button opens two new windows with the response prediction and path contribution plots. In this way the figures can be resized and saved as .JPG pictures.

“Condition number” button opens a new figure displaying the condition number of the matrices used in the analysis. This helps the user determine how uncertain the prediction and path contribution analysis is.

“View Forces” button opens a new window (Figure A17) that allows the user to inspect the identified forces.

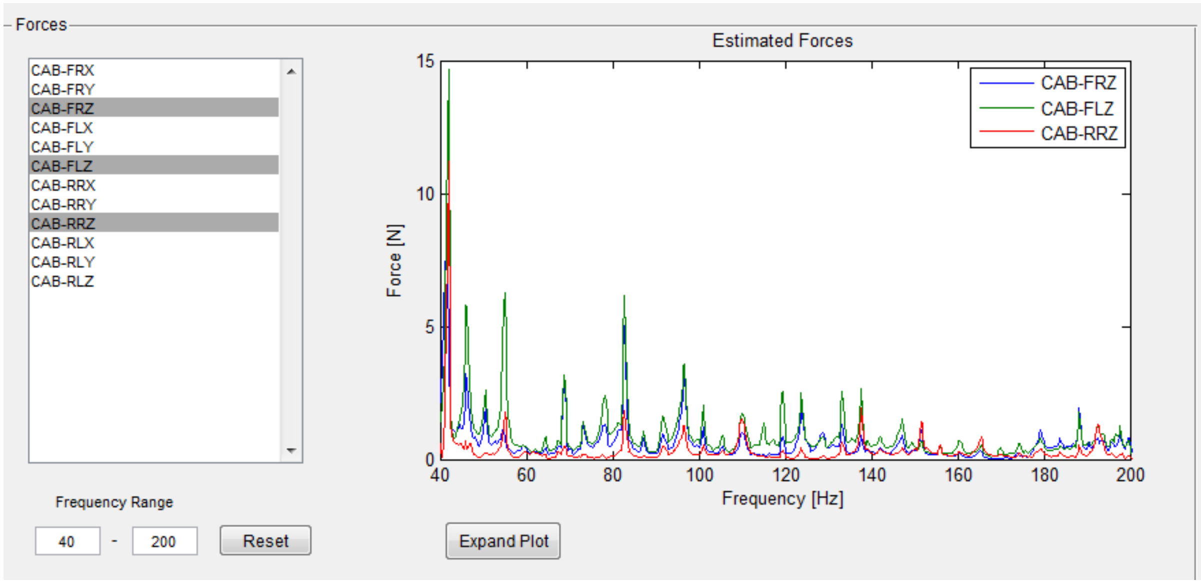

Figure A 17: Predicted forces display interface

"Detailed Contribution" button will open a new figure that contains 3 different plots: Force // Transfer Functions // Path Contribution. The purpose of this plot is to help the user identify the reason for obtaining a peak in the Path Contribution Plot. Since the Path Contribution= Force x Tr. Function, the user can see if a peak in the Path contribution is caused by high force or because of the Transfer Function.

If the problem is a big force then the problem can be solved by modifying the structure before the passive side of the path measured. If the problem is caused by a peak in the Transfer Function then the problem can be solved by modifying the structure between the passive side of the path and the receiver.

The following example is given: Front Left X and Rear Left Y mounts appear to contribute to the vibration level on the steering wheel in Z direction at 55 Hz (Figure A18).

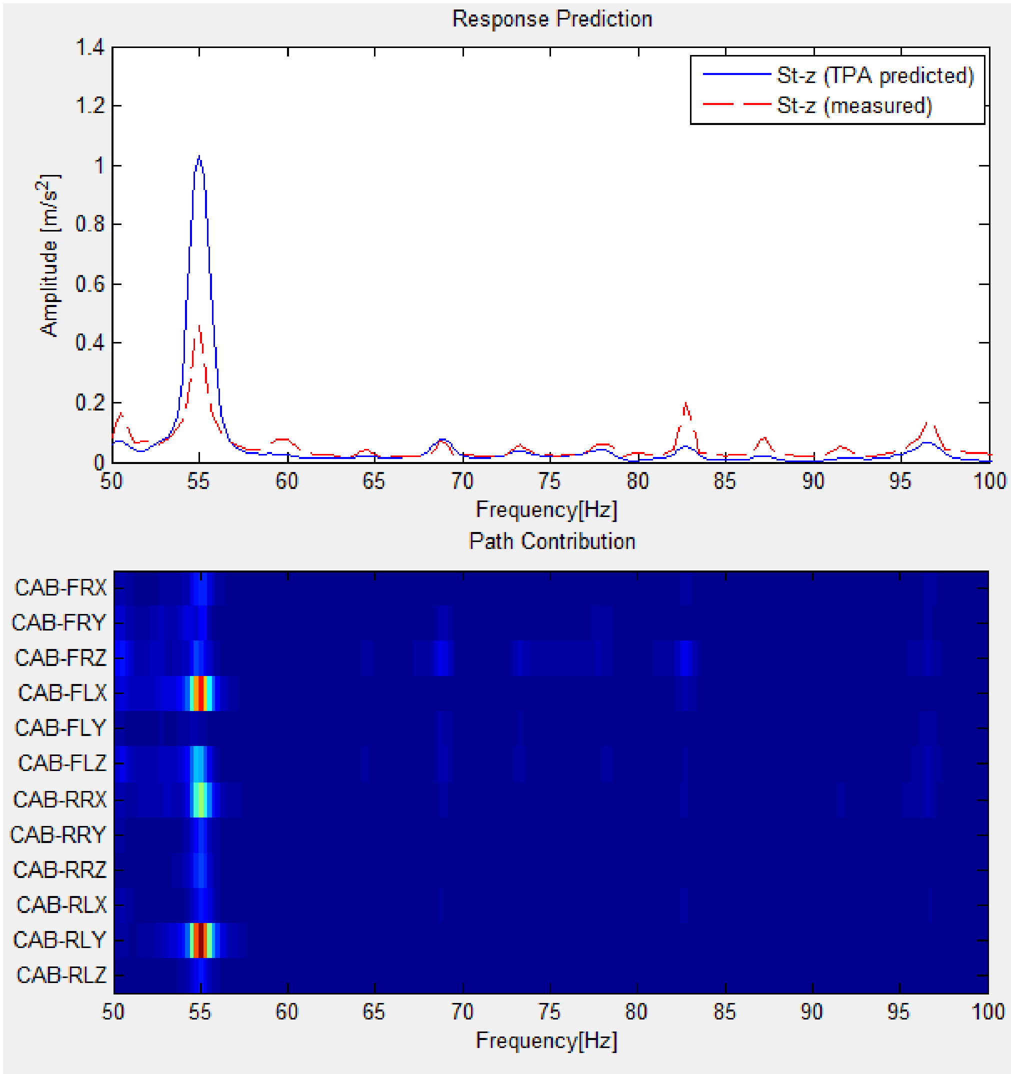

Figure A 18: Example for identifying if a high peak is caused by transfer function or high force

After opening the "Detailed contribution Plot" we can see that the contribution at the FLX path is given mostly by the force acting on the path. At the RLY path contribution, the Transfer function RL<->Steering Wheel Z is also contributing (Figure A19). The overall problem can be solved by reducing any of the contributing elements.

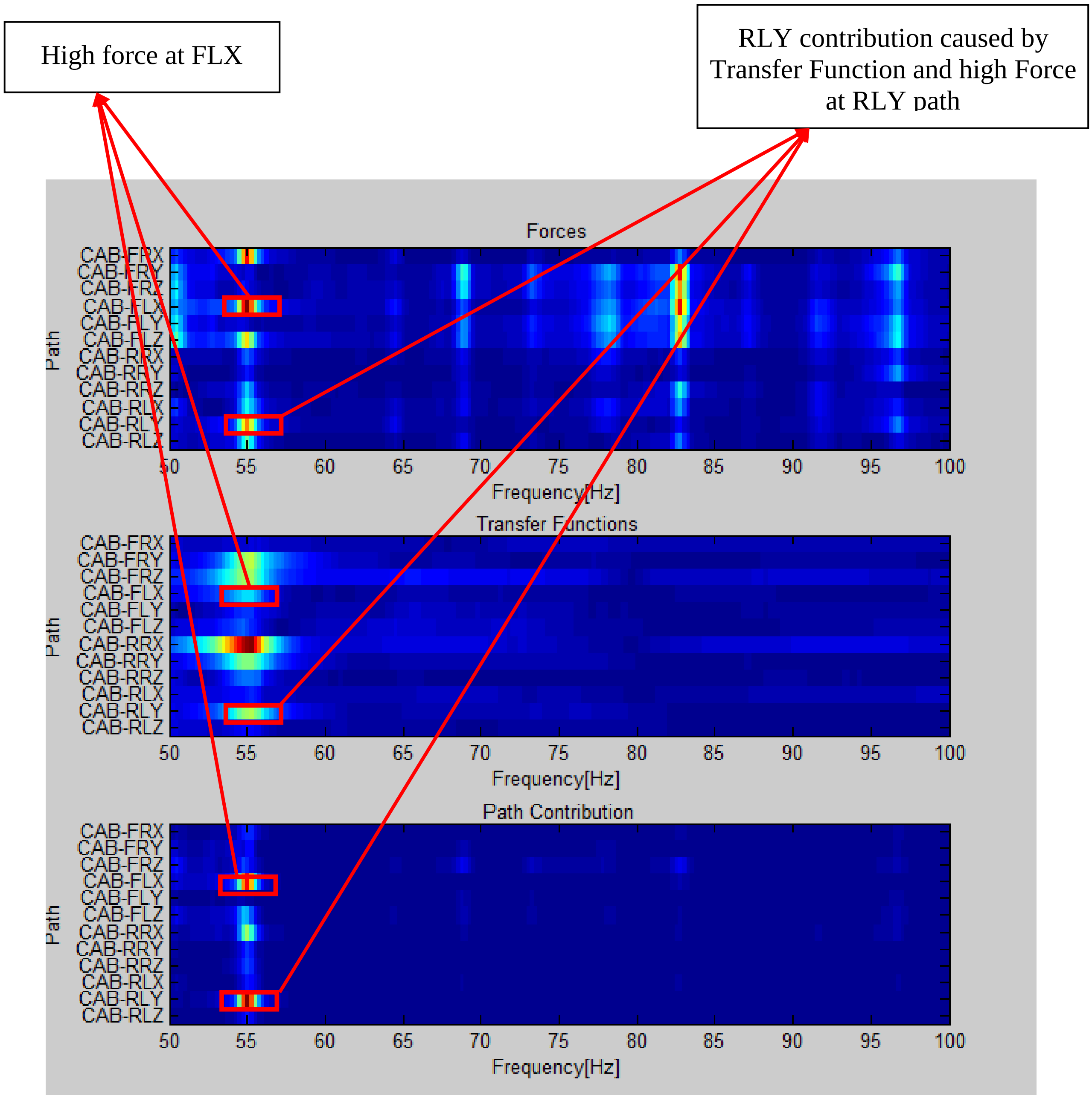

Figure A 19: Detailed Contribution Plot

“Export Force Data” button creates an excel file in a newly created “exported_files” subfolder. The excel file will contain the identified forces data.

“Export Contribution Data” button creates an excel file in a newly created “exported_files” subfolder. The excel file will contain the data from the Contribution Plot.